Applied Energy 283 (2021) 116201

Contents lists available at ScienceDirect

Applied Energy

journal homepage: www.elsevier.com/locate/apenergy

Spatial flexibility in redispatch: Supporting low carbon energy systems with Power-to-Gas

Bobby Xiong [a,b,*], Johannes Predel [a,b], Pedro Crespo del Granado [a,**], Ruud Egging-Bratseth [a]

[a] Department of Industrial Economics and Technology Management, Norwegian University of Science and Technology (NTNU), Trondheim, Norway
[b] Technische Universität Berlin (TU Berlin), Berlin, Germany

ARTICLE INFO

Keywords:
Power-to-Gas
Flexibility
Redispatch
Congestion management
Renewable energy
Sector coupling

ABSTRACT

The energy transition faces the challenge of increasing levels of decentralised renewable energy injection into an infrastructure originally laid out for centralised, dispatchable power generation. Due to limited transmission capacity and flexibility, large amounts of renewable electricity are curtailed. In this paper, we assess how Power-to-Gas facilities can provide spatial and temporal flexibility by shifting pressure from the electricity grid to the gas infrastructure. For this purpose, we propose a two-stage model incorporating the day-head spot market and subsequent redispatch. We introduce Power-to-Gas as a redispatch option and apply the model to the German electricity system. Instead of curtailing renewable electricity, synthetic natural gas can be produced and injected into the gas grid for later usage. Results show a reduction on curtailment of renewables by 12% through installing Power-to-Gas at a small set of nodes frequently facing curtailment. With the benefits of decentralised synthetic natural gas injection and usage, we exploit the advantages of coupling the two energy systems. The introduction of Power-to-Gas provides flexibility to the electricity system, while contributing to a higher effective utilisation of renewable energy sources as well as the natural gas grid.

1. Introduction

With the ongoing and future expansion of Renewable Energy (RE) sources, the amount of decentralised, intermittent electricity is increasing in the transmission grid. Historically, conventional power plants have been placed strategically, i.e., close to load centres. However, RE units are installed where their generation potential is maximised given the geographic weather conditions. Especially large amounts of wind generated electricity in areas with modest power consumption have to be transported to locations with high demand (industrial zones and densely populated areas).

In Germany, this has pushed transmission grids to their operational limits. With the task of maintaining a stable grid and maximising RE infeed in the generation mix, the costs for overall Congestion Management (CM) have increased during past years to almost a billion Euro annually (Fig. 1a).

To alleviate line congestion, Transmission System Operators (TSOs) rely on applying redispatch measurements. Current redispatch procedures often result in curtailing RE in front of the congested transmission lines and increasing electricity output of conventional, dispatchable power plants behind the curtailed lines. While the volumetric share of RE curtailment is lower than redispatch (Fig. 1b), its cost share in CM has grown from around half in 2015 to more than three quarters in 2019 (Fig. 1a). The curtailment of RE sources and upregulation of conventional power generation conflict with the goal of a low carbon energy system. As such, we can see curtailment of RE as an indication of lacking flexibility in electricity systems. Due to the decentralised nature of RE and the resulting geographical imbalances of load and generation, we refer to this type of flexibility as spatial flexibility.

In this paper, we consider curtailed renewable electricity as unused potential. In the long term, large-scale grid expansions can be expected to provide significant additional flexibility [6]. However, it will often take many years until additional capacity will be available. Meanwhile, flexibility potentials that could be provided by other energy sectors have not been explored to their full potential. In this regard, stronger cross-energy sector integration is a central pillar to more efficiently use existing infrastructure and technologies. In recent years, we have seen a growing interest in Power-to-Gas (PtG) as a promising technology to couple the electricity and gas sectors (Table 1). Rather than curtailing

* Corresponding author at: Technische Universität Berlin (TU Berlin), Berlin, Germany.
** Corresponding author.
E-mail addresses: b.xiong@tu-berlin.de (B. Xiong), pedro@ntnu.no (P. Crespo del Granado).

[1] Power-to-Gas (PtG) is composed of two consecutive process steps. During the first step, electrolysis, electricity is used to split water into hydrogen and oxygen [40]. In a second step, methanation, Synthetic Natural Gas (SNG) is produced. The SNG can directly be injected into the gas grid [66].

https://doi.org/10.1016/j.apenergy.2020.116201
Received 30 June 2020; Received in revised form 3 November 2020; Accepted 8 November 2020
Available online 26 November 2020

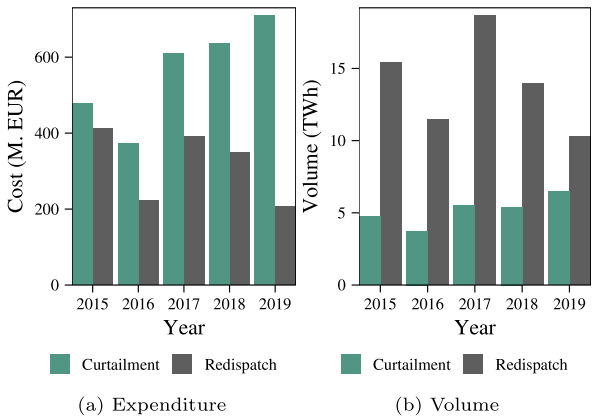

Fig. 1. Volume and expenditures for redispatch and curtailment from 2015 to 2019 in Germany BNetzA [1–5].

renewable infeed, the electricity may be used to produce carbon-neutral Synthetic Natural Gas (SNG) to replace conventional natural gas.[1] As such, PtG could provide flexibility by shifting pressure from the electricity to the gas system. Since natural gas usage in Europe has been declining, and is foreseen to decline further, the gas grid will be able to accommodate large amounts of SNG.

In this paper, we focus on assessing the potential of PtG in congestion management with the underlying main research questions:

- To what extent can PtG provide flexibility in redispatch?
- Which factors drive SNG production when PtG is used to reduce curtailment and redispatch volumes?

To address these questions, we have developed a two-stage, techno-economic Linear Program (LP) model. The first stage Economic Dispatch (ED) model implements the Day-Ahead (DA) spot market. Based on the first-stage market results, the second-stage CM model resolves transmission line congestions through redispatch measures. In a variant, we allow PtG as an option for spatial flexibility in the CM.

The following section reviews recent literature with a focus on flexibility in electricity systems. Next, in Section 3, we introduce the PtG technology, including its two key components electrolysis and methanation, and review PtG projects in Germany. In Section 4, we present our mathematical model formulations and underlying assumptions for the ED and CM while Section 5 presents the open-access data used. In Section 6, we discuss results, and perform sensitivity analyses for variations in PtG system efficiency, RE share, and CO_2 price in Section 7. We summarise and draw conclusions in Section 8.

2. The importance of spatial flexibility

When considering ancillary services, the term flexibility is rather used to address balancing energy instead of redispatch. Yet, in both types of ancillary services, flexibility is needed to secure a stable and reliable grid. Flexibility is often described as the ability to react to imbalances between load an generation [7,8]. Imbalances can occur both on demand and supply side [9] as well as due to factors external to the power system [10,11]. From a technical perspective, in an electrical grid flexibility is required to maintain frequency and voltage at desired levels.

To reconcile differences between generation and demand, TSOs procure balancing capacity in the balancing market. Prequalified flexibility providers can offer their flexibility to the TSO, who decides based on price and location which options to use. The type of flexibility can be differentiated by type (positive or negative) and duration (primary, secondary, tertiary) [12].[2] Different flexibility technologies exist for both demand and supply-side [13–15], as well as storage [13,16], and curtailment [9,17].

On the other hand, congestion management is used to alleviate congestion in the grid, and includes redispatch and feed-in management. From a regulatory and application-oriented point of view, it is necessary to strictly separate balancing energy and congestion management [18]. In order to prevent congestion, the TSO is allowed to reduce generation of qualified power plants before and increase generation after the congested lines. The term redispatch is used for dispatchable power plants. In case RE facilities have to reduce their output, the regulations for feed-in management, i.e., curtailment of RE, apply.

Calculations for redispatch measures take place before the intraday market [19]. Each balance-responsible party has to send their result of the day-ahead auction for their balancing group to the TSO. Based on these results and on own forecasts, the TSO selects which power plants should be available for redispatch. Due to the separation of the balancing markets and congestion management, a conflicting management of power plants may occur. As such, the mandated adjustments in balancing and in redispatch may interfere with each other [20,21]. Part of the discrepancy is due to a lack in communication between transmission and distribution grid operators as well as between TSO and affected power plants. Better communication and larger reserves for balancing would resolve this [20]. Additionally, a more integrated view on flexibility and redispatch could be beneficial, especially in light of the foreseen phase-out of dispatchable nuclear and coal-fired generation capacities [18].

Obligations for the curtailment of RE are described in §14 EEG. Feed-in management is the “last resort” by TSOs to prevent congestion and only allowed when all other options cannot be successful. This ensures that the largest possible volume of RE is used. Curtailment volumes are based on the TSO’s own forecasts. The TSO is obliged to communicate curtailment volumes to power plant owners one day prior to the occurrence, unless their need could not be foreseen reasonably (§14, 2 EEG). As such, the timing and volume of curtailment relies largely on the forecasting accuracy 24-hours ahead by the TSO. Yet, the time between mandated curtailment and actual curtailment of the RE facility is unknown. Only the affected facility, the start and end time of the curtailment, and the reason are available.

There are different classifications of the time intervals between information availability and start time of the congestion management measure. dena [20] distinguishes between long-, mid- and short-term measures (intraday changes due to changes in wind speed and solar radiation, which may be communicated right before delivery). Nabe and Neuhoff [18] even speak of “short-term redispatch measures”, occurring during the intraday market. Hadush and Meeus [21] point out different states of reaction of the TSO from green (no need for any congestion management) to red (curtailment or other technical measures are needed). Forecast errors and their impact on redispatch have been analysed by Kloubert et al. [29]. They propose to implement an intraday redispatch market, which would reduce overall redispatch cost, since forecast errors are generally smaller closer to delivery time. Such short-term deviations from the day-ahead redispatch have to be taken into account when analysing concepts for curtailment reduction. Under perfect information and favourable conditions, curtailment may be planned like redispatch immediately after the day-ahead and well before the intraday market. In that case, flexibility may not be an important factor to reduce curtailment. However, due to the fluctuating nature of RE and their growing installed capacity, the available measures must be flexible enough to cope with short-term changes intraday and physically close enough to where curtailment is needed.

[2] For Germany, the anonymous bids and the outcomes of the balancing market can be found on regelleistung.net.

Table 1
Overview of PtG projects in Germany.

Name	Year	Status	Electrolysis	Methanation	Max input (kW_{el})	Min input	Max output (N m^3/h)[a]	Eff.	Ramping	Source
Exytron Compact PtG	2019	Active	AEL	Catalytic	62.5	n.a.	2.5	0.9[b]	n.a.	dena [22]
Exytron Alzey	2019	Active	AEL	Catalytic	500	n.a.	n.a.	n.a.	n.a.	dena [22]
Store&Go at Falkenhagen	2018	Active	AEL	Catalytic	2000	n.a.	57	0.58	n.a.	dena [22] and StoreandGo [23]
BioPower2 Gas	2016	Ended	PEM	Biological	300	n.a.	15	n.a.	n.a.	dena [22], Aryal et al. [24] and Heidrich et al. [25]
Exytron Demo	2015	Active	AEL	Catalytic	21	n.a.	1	0.9[b]	n.a.	dena [22]
Methanation at Eichhof	2015	Ended	n.a.	Biological	25	n.a.	4	n.a.	n.a.	dena [22]
Audi e-gas	2013	Active	AEL	Catalytic	6000	n.a.	325	0.54	≥ 1 MW per 5 min	Ghaib and Ben-Fares [26]
PtG at Eucolino	2012	Active	n.a.	Biological	108	n.a.	5.3	n.a.	n.a.	dena [22]
Helmeth	2012	Ended	SOEC	Catalytic	n.a	20%	60 kW_{th}	0.76[b]	n.a.	Gruber et al. [27]
PtG 250	2011	Ended	AEL	Catalytic	250	70%	n.a.	0.496	n.a.	Zuberbuehler [28]

[a]A standard cubic metre (N m^3) is the amount of gas (in this case CH_4 at 1.01325 bar and 273.15 K).
[b]Including heat utilisation of the methanation process.

PtG may offer such a solution. Naturally, benefits of additional flexibility options for redispatch depend on costs, efficiency, and availability. High costs (above € 100/MWh), limited capacity, and short availability periods all undermine the potential [30]. A feasible option needs to be cost-efficient and available throughout periods with curtailment activity.

In contrast to flexibility in balancing markets that are energy only, flexibility for redispatch must account for two different location at the same time, i.e., before, and after a congested grid element. To a certain extent, negative flexibility (or load reduction) before and positive flexibility (load increase) after the congestion may be provided. However, this would not only decrease the flexibility reserves for balancing markets, but also increase the need for real-time adjustments [20]. If these two locations lie in different balancing groups, this may cause conflicts with balancing measures in both groups. Therefore, load reduction may contribute to the conflict potential between balancing markets and congestion management.

To refer to the twofold locational impact, described above, we denote flexibility for congestion management as *spatial flexibility*. Spatial flexibility is highly related to other types of flexibility measures, such as grid extensions. Grid reinforcements are necessary to cope with the challenges of decentralised energy generation [11,13]. Additionally, the size of the system can have a beneficial effect on flexibility. Huber et al. [8] point out that connecting smaller areas reduces the need for flexibility as uncorrelated local imbalances can compensate each other. While grid extension may reduce the overall need for flexibility [31], ongoing grid projects face great opposition in the public, resulting in legal challenges and long planning and project lead times [32].

In contrast, technologies that use already existing infrastructures are likely to suffer much less opposition. By shifting an energy carrier from one infrastructure to the other (e.g., from the electricity to the gas grid), flexibility options in both systems can be used. Pilpola and Lund [33] and Brown et al. [34] investigate how renewable infeed can be increased through flexibility by sector coupling. On the demand side, technologies include PtG, Power-to-Heat and smart charging of electric vehicles. On the supply side they incorporate wind power curtailment and Vehicle-to-Grid [11,34,35]. Flexibility by PtG, and possible locations have been analysed by Haumaier et al. [36]. In one of their scenarios, surplus wind onshore generation is used to produce H_2 and SNG. They conclude that, while the potential for PtG exists, consumer charges, electricity tariffs, and taxes, pose a barrier to PtG becoming a feasible, competitive flexibility option. To the best of our knowledge, explicitly considering the spatial dimension in flexibility provided by combining PtG with gas-fired power plants has received limited attention in the literature.

Therefore, we propose to analyse the potential of PtG in redispatch. Spatial flexibility is central to use otherwise curtailed renewable electricity by producing SNG. After injection to the gas grid, it can then be used by connected Gas-fired Generation (GfG) units to generate electricity. In fact, only in combination with GfG units, PtG can be seen as spatial flexibility option. In order to cope with "short-term redispatch" measures, PtG as a sector coupling technology needs to be flexible enough to allow unforeseen variation in RE infeed during the intraday market. Being able to do so, PtG may be a viable technology to reduce RE curtailment.

Table 2
Overview of electrolysis parameters.

Source	Electrolysis	Efficiency (%)	Ramping (%/s)	Min. input (%)
Thema et al. [38]	n.a.	70	n.a.	n.a.
Milanzi et al. [44]	AEL	74	33	20–40
	PEM	67	10	0–10
	SOEC	82	n.a.	n.a.
Quarton and Samsatli [39]	AEL	73	n.a.	n.a.
	PEM	76	n.a.	n.a.
	SOEC	≥ 80	n.a.	n.a.
Götz et al. [45]	AEL	70	n.a.	n.a.
	PEM	70	n.a.	n.a.
Schiebahn et al. [43]	AEL	67	10	20–40
	PEM	67	10–100	5–10
Sterner et al. [46]	n.a.	64–77	n.a.	n.a.

3. Power-to-Gas applications in Germany

Globally, the majority of PtG projects is located in Germany [37–39]. Table 1 gives an overview of past and ongoing PtG projects in Germany. For most project, the sources do not reveal all technical parameters, such as ramping times and minimum input. Therefore, we present additionally the state-of-the-art on both electrolysis and methanation (Table 2). The most common technologies chosen for electrolysis are Alkaline Water Electrolysis (AEL) and Polymer Electrolyte Membrane (PEM). Although Solid Oxide Electrolyte Electrolysis (SOEC) can reach higher efficiency (more than 80 %) it is still in a laboratory stage only. Its main challenge is to mitigate the impact of high temperatures on the used materials [40]. Recently, the Helmeth project has shown promising results by coupling SOEC with a methanation process and using excess heat of the latter to reuse it in the process, hence increasing the overall efficiency [27]. Both AEL and PEM are flexible and able to increase power input within seconds. Some electrolysis units have been used for secondary control reserves, which requires the ability to ramp-up to at least one MW in five minutes [41]. In terms of flexibility and application in control reserve markets, the PEM technology seems most promising [42]. While AEL needs to run at minimum loads of around 20–40 % [43], PEM can be operated at less than 10 % [43,44].

Most current German PtG projects rely on AEL rather than PEM (Table 1). This indicates that the units were not intended to provide

Table 3
Overview of methanation parameters.

Source	Methanation	Efficiency (%)	Min. input (%)
Salomone et al. [48]	Catalytic	83 .	n.a.
Boudellal [37]	n.a. n.a.	≥ 80 93	n.a. n.a.
Schmidt et al. [49]	Catalytic	70–85	n.a.
Milanzi et al. [44]	Cath. & Biological	80[b] 78[a]	0.25 n.a.
Götz et al. [45]	Catalytic	78	0.1–0.4
Schiebahn et al. [43]	Catalytic	83	n.a.

[a]Literature median.
[b]Project median.

flexibility, but rather to produce SNG at lowest cost, as lifetime and investment cost are the relative advantages of AEL [45]. For methanation, both biological and catalytic processes are used. In a biological methanation the produced hydrogen is often used as a co-substrate to increase biogas output of existing biogas plants [47]. Hydrogen can be used to accelerate biological processes and increase biogas purity [24] and is mostly used in small-scale applications [45,47]. For units with the highest installed capacity, i.e., Store&Go Falkenhagen and Audi e-gas, a catalytic approach is used rather than a biological. Further review of methanation processes (Table 3) shows the advantage of catalytic methanation: much higher efficiencies up to the theoretical maximum efficiency of 83 % of this exothermic reaction [43,48]. System efficiencies higher than 83 % can be achieved by making use of the waste heat [43,44].

A challenge with catalytic methanation is heat management as the reaction temperature needs to be above 700 °C. The minimum load for catalytic methanation is at around 20–40 % [50]. Below 20 %, the process becomes very inefficient and the produced SNG has low quality [50]. Unfortnately, no sources reveal technical data regarding start up times and minimum load, which should be accounted for in a model focusing on flexibility.

When considering flexibility of a PtG unit, ramping time and minimum load requirements are the main determinants. On these aspects, PEM has the most favourable characteristics and is therefore most suitable to deal with electricity input variations. To achieve high efficiency and sufficient SNG purity, catalytic methanation seems appropriate. To further increase the flexibility and cost-effectiveness of the PtG unit the electrolysis process output and the methanation process input can be decoupled using storage capacity for hydrogen [51]. This allows the methanation to run at higher and less fluctuating levels. We implicitly assume such a storage to be available with high enough capacity.

4. Model

We implement a two-stage LP model, consisting of an ED and a CM model including transmission constraints. To model the decoupled procedure of the DA market and CM, we propose sequential market clearing, followed by hourly redispatch at a limited foresight of 24 h. This structure reflects the DA spot market and current cost-based redispatch mechanism in Germany. Sequencing allows us to analyse longer periods day by day in a rolling horizon fashion. A schematic overview is presented in Fig. 2. The short vertical arrows represent the individual 24 h of a day which are considered in the CM model. We include a list of the model terminology, including sets, variables, and parameters Appendix A. Variables are displayed in uppercase italic, while parameters are written in lowercase roman.

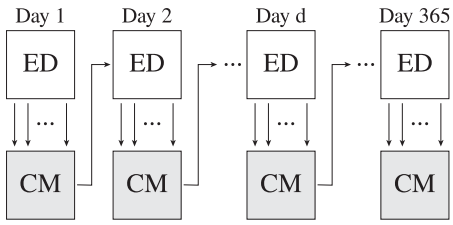

Fig. 2. Schematic overview on sequential model runs including ED and CM.

4.1. Model assumptions

With the objective of this paper to assess the potential of PtG in redispatch, we make some assumptions to maintain a balance between technical accuracy, computational complexity, and result quality. In the following we briefly present and explain the model assumptions.

Ramping. The ramp rate describes a thermal power plant's ability to increase and decrease output per time (e.g., in MW/min). For rotating generation units (coal, nuclear, hydro, etc.) ramp-rates range from 2 % to 15 % per minute of their maximum output [52]. As such, with an hourly modelling resolution, this would translate into possible ramp rates of 100 % per hour, making a ramping constraint non-binding. At an hourly level, we can hence neglect ramping constraints. This does not impact the model results but reduces the number of constraints by $2 * \mathcal{G} * (8760 - 1)$ and thus calculation complexity. Note that including ramping in models with quarter-hourly or minute resolutions would significantly impact the model outcome.

No commercial cross-border exchange. Including historic cross-border exchange time series as a fixed parameter to the model directly translates into an increase in load in times of export and a decrease in times of import (Eq. (2)). As such, an electricity export would yield an increased Market Clearing Price (MP). However in reality, if electricity is exported from a country A to country B in a particular hour, a lower zonal MP in country A than in country B is indicated. For this reason we do not include historic cross-border trade. Alternatively, modelling the market and subsequent redispatch for Germany and all neighbouring countries would require larger data sets and computational times which are beyond the technical and contextual scope of this paper. As such, to be able to narrow down the potential impact of PtG and to keep computational times within acceptable limits, we only determine the ED and CM on a national level. We point out that by neglecting cross-border exchange, congestion that may be induced or alleviated through trade on interconnectors are not represented.

Virtual SNG storage. To keep track of the amount of SNG in the gas grid (i.e., produced but not used yet), we assume the presence of a single virtual SNG storage. All PtG units can inject into the storage and all GfG units can withdraw SNG. In future research, this assumption may be substituted by modelling the gas grid.

4.2. Day-ahead economic dispatch

The ED model minimises total system costs for generation while considering Marginal Cost (MC), market clearing, and Pumped Hydroelectric Storage (PHS) constraints. Given uniform pricing on the DA spot market, a single copper plate is assumed, i.e., physical transmission line constraints are neglected in the bidding process. From this optimisation step, we obtain total system costs and a cost-minimal dispatch for all generation units. We deliberately exclude binary variables, such as unit commitment, to obtain the market price as the dual to the market clearing constraint (Eq. (2)).

Objective function. The objective function (Eq. (1)) minimises total generation costs summed up over all technologies and the total, 24 h time horizon.

$$\min_{P_{g,t}^{DA}} \sum_{t} \sum_{g} \mathrm{c}_{g}^{\mathrm{mc}} P_{g,t}^{DA} \tag{1}$$

Market clearing. The market clearing constraint (Eq. (2)) ensures that demand is satisfied by the generation units at all times.

$$\sum_{g} P_{g,t}^{DA} - \sum_{n} \mathrm{d}_{n,t}^{\mathrm{load}} = 0 \quad , t \in \mathcal{T} \tag{2}$$

Power generation. A generation unit can only operate within a certain range (Eq. (3)). The output of a generation unit is lower-bound by must-run obligations and upper-bound by its installed capacity.

$$\mathrm{p}_{g}^{\min} \leq P_{g,t}^{DA} \leq \mathrm{p}_{g}^{\max} \quad , g \in \mathcal{G}, t \in \mathcal{T} \tag{3}$$

PHS. A PHS is defined by its maximum pumping (Eq. (4)), generating power (Eq. (5)) and storage capacity (Eq. (6)). Its storage level can never exceed the maximum capacity and is calculated based on the previous storage level, plus electricity demand and minus generation of the previous period (Eq. (7)).

$$D_{s,t} \leq \mathrm{p}_{s}^{\max} \quad , s \in \mathcal{S}, t \in \mathcal{T} \tag{4}$$

$$P_{s,t}^{DA} \leq \mathrm{p}_{s}^{\max} \quad , s \in \mathcal{S}, t \in \mathcal{T} \tag{5}$$

$$L_{s,t} \leq \mathrm{l}_{s}^{\max} \quad , s \in \mathcal{S}, t \in \mathcal{T} \tag{6}$$

$$L_{s,t} = L_{s,t-1} - P_{s,t-1}^{DA} + \eta_{\mathrm{s}} D_{s,t-1} \quad , s \in \mathcal{S}, t \in \mathcal{T} : t > 1 \tag{7}$$

Non negativity. Eq. (8) ensures that the power output, PHS pumping and storage level can never be negative.

$$P_{g,t}^{DA} \geq 0 \quad , g \in \mathcal{G}, t \in \mathcal{T} \tag{8}$$

$$P_{s,t}^{DA} \geq 0 \quad , s \in \mathcal{S}, t \in \mathcal{T} \tag{9}$$

$$D_{s,t}^{DA} \geq 0 \quad , s \in \mathcal{S}, t \in \mathcal{T} \tag{10}$$

$$L_{s,t}^{DA} \geq 0 \quad , s \in \mathcal{S}, t \in \mathcal{T} \tag{11}$$

4.3. Congestion management

Following a previous formulation by Kunz and Zerrahn [53], we implement a CM model which includes Direct Current (DC) power flow grid constraints and decisions based on the market results, i.e., the MP and dispatch for each hour. In this modelling step, we calculate a system-wide cost minimal redispatch, i.e., upwards and downwards adjustments of dispatchable power plants and curtailment of RE units, required to meet the physical constraints of the transmission grid.

Objective function. The CM model minimises the total cost for redispatch and feed-in management (Eq. (12)). Following the formulation by Kunz [54, 7] and based on current remuneration schemes [19,55] redispatch is profit-neutral: Power plants that increase their output to their previous bid are reimbursed by their MC. At the same time, an output decrease of a power plant is compensated by its lost profit, i.e., the difference of the MP at a time t minus its MC. We include additional costs for an increase of output by PHS accounting for efficiency losses. In addition, we include costs for lost load.

$$\min_{\Delta P_{g,t}^{+}, \Delta P_{g,t}^{-}} \sum_{t} \sum_{n} \left[\sum_{g} \left(\mathrm{c}_{g}^{\mathrm{mc}} \Delta P_{g,t}^{+} + (\overline{\Psi}_{t} - \mathrm{c}_{g}^{\mathrm{mc}}) \Delta P_{g,t}^{-} \right) + \sum_{s} \frac{\overline{\Psi}_{t}}{\eta_{\mathrm{s}}} \Delta P_{s,t}^{+} + \mathrm{c}^{\mathrm{VOLL}} P_{n,t}^{lost} \right] \tag{12}$$

In the CM model, we use variables $P'_{g,t}$ to denote the composition of the day-ahead dispatch, plus upwards and downwards power adjustments in the CM model (Eq. (13)).

$$P'_{g,t} = \overline{P}_{g,t}^{DA} + \Delta P_{g,t}^{+} - \Delta P_{g,t}^{-} \tag{13}$$

Nodal balance and power injection. The market clearing constraint from the ED now has to hold at each node (Eq. (14)). Power injection at a node n is defined as the net difference between all connected generation (positive) and load (negative). Using the susceptance entry on the admittance matrix, the voltage angles are linked to the nodal injection (Eq. (15)).

$$\sum_{g} P'_{g,t} - \mathrm{d}_{n,t}^{\mathrm{load}} = P_{n,t}^{inj} \quad , n \in \mathcal{N}, t \in \mathcal{T} \tag{14}$$

$$\sum_{m} b_{n,m} (\Theta_{n,t} - \Theta_{m,t}) = P_{n,t}^{inj} \quad , n \in \mathcal{N}, t \in \mathcal{T} \tag{15}$$

Line power flow. Using the line reactance and voltage angles at the from-node n and to-node m, we calculate the power flow on a transmission line (Eq. (16)). The line flow must not exceed its thermal capacity limit including the Transmission Reliability Margin (TRM) at all times (Eqs. (17) and (18)). The parameter trm is a value between 0 and 1. This constraint holds true in both flow directions.

$$x_{n,m}^{-1} (\Theta_{n,t} - \Theta_{m,t}) = P_{n,m,t}^{flow} \quad , n, m \in \mathcal{N} : n \neq m, t \in \mathcal{T} \tag{16}$$

$$P_{l,t}^{\mathrm{flow}} \leq p_{l}^{\max} (1 - \mathrm{trm}) \quad , l \in \mathcal{L}, t \in \mathcal{T} \tag{17}$$

$$-\left[p_{l}^{\max} (1 - \mathrm{trm}) \right] \leq P_{l,t}^{\mathrm{flow}} \quad , l \in \mathcal{L}, t \in \mathcal{T} \tag{18}$$

Power generation. Without the use of binary variables, we can avoid a power plant being adjusted both upwards and downwards at the same time step by adjusting the constraint for power generation limits.

$$\overline{P}_{g,t}^{DA} + \Delta P_{g,t}^{+} \leq \mathrm{p}_{g}^{\max} \quad , g \in \mathcal{G}, t \in \mathcal{T} \tag{19}$$

$$\mathrm{p}_{g}^{\min} \leq \overline{P}_{g,t}^{DA} - \Delta P_{g,t}^{-} \quad , g \in \mathcal{G}, t \in \mathcal{T} \tag{20}$$

$$P_{s,t}^{DA} + \Delta P_{s,t}^{+} \leq \mathrm{p}_{s}^{\max} \quad , s \in \mathcal{S}, t \in \mathcal{T} \tag{21}$$

Non negativity. Non-negativity constraints (Eq. (22)) also apply here, with $\overline{P}_{g,t}^{DA}$ being replaced by $P'_{g,t}$.

$$P'_{g,t} \geq 0 \quad , g \in \mathcal{G}, t \in \mathcal{T} \tag{22}$$

4.4. Power-to-Gas extension

We extend the CM model from Section 4.3 with PtG facilities at all nodes where RE units feed into the grid. To observe how much SNG is used, we introduce an additional power generation variable $P_{e,t}^{PtG}$ for all GfG units.

Objective function. Fuel costs for PtG units occur when electricity is used to produce SNG. As such, the MP has to be paid, accounting for efficiency losses during electrolysis and methanation. To use SNG to generate electricity, the variable Operation and Maintenance (O&M) costs of GfG units are accounted for (Eq. (23)).

$$\min_{\Delta P_{g,t}^{+}, \Delta P_{g,t}^{-}, E_{g,t}} \sum_{t} \sum_{n} \left[\sum_{g} \left(\mathrm{c}_{g}^{\mathrm{mc}} \Delta P_{g,t}^{+} + (\overline{\Psi}_{t} - \mathrm{c}_{g}^{\mathrm{mc}}) \Delta P_{g,t}^{-} \right) + \sum_{s} \frac{\overline{\Psi}_{t}}{\eta_{\mathrm{s}}} \Delta P_{s,t}^{+} + \mathrm{c}^{\mathrm{VOLL}} P_{n,t}^{lost} + \sum_{r} \frac{\overline{\Psi}_{t}}{\eta_{\mathrm{E}} \eta_{\mathrm{M}}} D_{r,t}^{PtG} + \sum_{r} \mathrm{c}_{e}^{\mathrm{OM}} P_{e,t}^{PtG} \right] \tag{23}$$

Power-to-Gas capacity. As an alternative to RE curtailment, PtG facilities can use the electricity. PtG facilities can only make use of remaining available output (volume of curtailment) of a solar PV or wind generation unit (Eq. (24)) or its capacity limit (Eq. (25)).

$$P'_{r,t} - D_{r,t}^{PtG} \leq \mathrm{p}_{r}^{\max} \quad , r \in \mathcal{R}, t \in \mathcal{T} \tag{24}$$

$$D_{r,t}^{PtG} \leq \mathrm{d}_{r}^{\max} \quad , r \in \mathcal{R}, t \in \mathcal{T} \tag{25}$$

SNG storage level. Efficiency rates from electrolysis and methanation are accounted for in the demand for electricity from the PtG unit. The storage level (Eq. (26)) is determined by the level at the end of the previous period, subtracted by what is withdrawn for power generation, plus the SNG produced by PtG units. At the beginning of the first modelling day, the SNG storage level is set to zero (Eq. (27)).

$$L_t = L_{t-1} - \sum_e \frac{1}{\eta_e} P^{PtG}_{e,t-1} + \eta_E \eta_M \sum_r D^{PtG}_{r,t-1} \quad ,t \in \mathcal{T} : t > 1 \tag{26}$$

$$L_1 = l^{init} \tag{27}$$

Gas-fired generation. As an alternative to using natural gas as input fuel, GfG units can use SNG in CM. However, SNG can only be used as long as it is available in the virtual storage (Eq. (28)), accounting for the individual thermal efficiency of GfG units.

$$\sum_e \frac{1}{\eta_e} P^{PtG}_{e,t} \le L_t \quad ,t \in \mathcal{T} \tag{28}$$

Nodal balance and power injection. The nodal power injection constraint needs to be adjusted to incorporate the electricity demand by PtG units and re-electrification of SNG in GfG units.

$$\sum_g P'_{g,t} + \sum_e P^{PtG}_{e,t} - p_d - \sum_r D^{PtG}_{r,t} = P^{inj}_{n,t} \quad ,n \in \mathcal{N}, t \in \mathcal{T} \tag{29}$$

Relations between the ED and CM (Eq. (13)), as well as nodal angles (Eq. (15)), line power flow constraints (Eqs. (16), (17), and (18)), remain unchanged.

Power generation. For conventional, non-GfG units and RE units, the constraints for generation limits stay the same (Eqs. (19) and (20)). For GfG units, the sum of power generation from fossil and SNG must not exceed its capacity limit (Eq. (30)).

$$\overline{P}^{DA}_{g,t} + \Delta P^{+}_{g,t} + P^{PtG}_{e,t} \le p^{max}_e \quad ,e \in \mathcal{E} :, t \in \mathcal{T} \tag{30}$$

Non negativity. In addition to Eq. (22), the electricity demand from PtG units (Eq. (31)) and generation from SNG can never be negative (Eq. (32)).

$$D^{PtG}_{r,t} \ge 0 \quad ,r \in \mathcal{R}, t \in \mathcal{T} \tag{31}$$

$$P^{PtG}_{e,t} \ge 0 \quad ,e \in E, t \in \mathcal{T} \tag{32}$$

4.5. Model implementation

We implement our linear program in the open-source language Julia (v.1.3.1), using the Julia for Mathematical Programming (JuMP) package. In addition, we have built an entire data evaluation toolchain in R (v.4.0.0) using ggplot2 and leaflet that allows us to visualise model results.

5. Data

We use an open access reference data set (version 1.0.0), which covers the entire German electricity, heat, and natural gas sector as of late 2015 [56]. For the purpose of performing an economic dispatch and subsequent redispatch, we extract data on electric load, installed capacities of conventional and RE generation units, transmission line capacities, resistance, and reactance, prepared by Weibezahn and Kendziorski [57]. In the following paragraphs, we provide a brief overview on the used data. To obtain more detailed insights on how the geospatial data was collected, we refer to the data documentation by Kunz et al. [58].

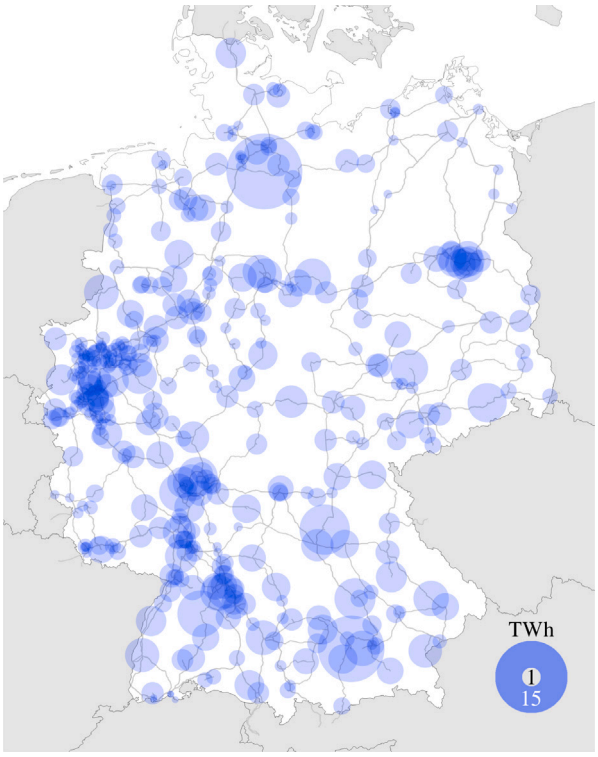

Fig. 3. Load distribution over a year. Circle area proportional to load. Transmission lines are displayed in grey colour.
Source: Own illustration based on Kunz et al. [56].

Table 4
Overview of transmission lines.

Voltage kV	Circuits #	Th. Capacity MW	Lines #
220	Single	490	228
220	Double	490	129
220	Triple	490	2
380	Single	1700, 2300	244
380	Double	1700, 2300	118
380	Triple	1700	3

5.1. Data overview

Transmission grid. The data set includes 724 multi-circuit AC transmission lines (Table 4).

Load. The total annual load of 540.339 TWh is distributed across 427 national nodes at hourly resolution (Fig. 3). Load centres are located in large metropolitan areas and the southwestern region of Germany.

Generation. The data set includes 613 individual thermal power plants and 33 PHS units, mapped to nodes. RE generation units are aggregated at nodal level. As of the end of 2015, the installed capacity of generation units in Germany totalled 197.4 GW, of which 93 GW are accounted by conventional thermal power plants, 20.6 GW by flexible RE power plants (biomass, Hydro Run-of-River (RoR), PHS, and geothermal) and 83.8 GW by intermittent RE generation units, such as wind and solar Photovoltaics (PV) (Table 5).

The generation of wind onshore, offshore, and solar PV is calculated using weather infeed data at hourly resolution [58]. A geospatial distribution of RE generation infeed is presented in Fig. 4.

Merit order. Marginal generation costs (Eq. (33)) are calculated based on power plant efficiency, fuel costs, variable O&M costs and emission

Table 5
Installed capacity and availability.

Fuel	Installed capacity (GW)	Average availability
Wind onshore	41.2	0.190
Wind offshore	3.3	0.259
Solar PV	39.3	0.096
Biomass	8.1	0.575
RoR	3.7	0.532
PHS	8.8	–
Geothermal	0.03	0.310
Natural gas	23.6	0.800
Nuclear	12.1	0.823
Lignite	20.9	0.774
Hard coal	28.6	0.720
Oil (light)	3.1	0.800
Oil (heavy)	0.6	0.800
Waste	1.6	0.700
Other fuels	2.5	0.530

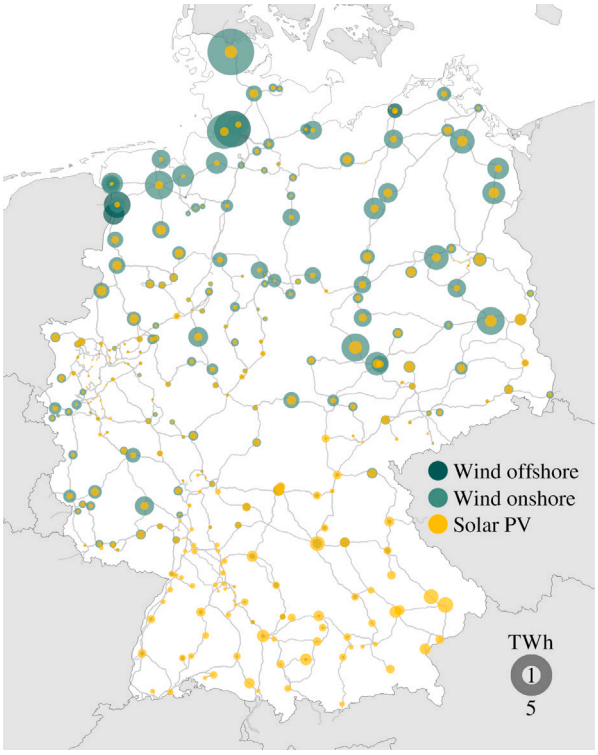

Fig. 4. Maximum electricity generation by intermittent RE source over a year.

factors (Table B.8). A CO_2 price of 7.59 €/t is used for the year 2015 [58].

$$c_g^{mc} = \frac{c^{fuel} + c^{CO_2}\lambda_g}{\eta_g} + c_g^{OM} \quad , g \in \mathcal{G} \tag{33}$$

Based on the installed capacities of RE units and conventional power plants of 2015 (Table 5) [58], this yields the following merit order (Fig. 5).

5.2. Data assumptions

In the following, we briefly present the assumptions within and beyond the data set used.

Must-run. While we have technically formulated must-run in the model, minimum generation obligations in the data set are not considered, i.e., $p_g^{min} = 0$. While some studies endogenously approximate must-run obligations from combined heat and power plants based on

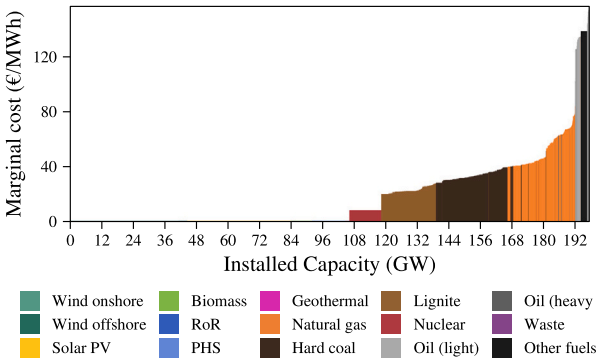

Fig. 5. ED merit order based on Kunz et al. [58].

heat demand, these methods require additional modelling [59]. In addition, the implementation of must-run generation is equivalent in reducing the remaining dispatch for endogenous optimisation. As such the merit order (Fig. 5) is shifted to the right, and by obtaining the MP from the dual to the market clearing condition, this yields a lower price. Meanwhile, must-run capacities are remunerated through individual, long-term contracts which we cannot replicate in the model. We further deliberately do not assume a flat fuel- or technology-specific must-run share [52] for two reasons: (i) This overestimates the redispatch volume required as basically all thermal generations might be redispatched to satisfy both must-run and transmission constraints; (ii) By including must-run, in some hours, a share of RE is curtailed in the ED already. Under these circumstances, more renewable electricity is available which may lead to an over-estimation of PtG. We point out that due to a lack of must-run obligations, which primarily concerns GfG units, our model underestimates the share of natural gas in the dispatch, given its position in the merit order (Fig. 5).

Availability of power plants. To adequately represent power plant outages, as well as scheduled and unscheduled shutdowns, we use fuel-specific, monthly availability factors provided by Kunz et al. [58]. Further calibration to historic data [60] is done by scaling down nuclear power plant availability.

PHS. Incorporating PHS and assessing a water value is a challenging topic on its own. As a direct result of cost-minimisation problems, there is no incentive to leave a PHS remaining storage level, i.e., the PHS storage level at the end of a modelling period is zero if not explicitly defined otherwise. To represent PHS in redispatch measures, we make the simplified assumption, that 80 % of the maximum PHS storage capacity is available for economic dispatch and 20 % for redispatch. We point out that this assumption can definitely be further improved. The German online grid transparency platform [61] provides data on redispatch volume by utility. In the case of PHS, data for the largest PHS utility is aggregated with RoR. Due to limited data available on the cost of electricity that PHS utilities have to pay, we further assume that an increase generation output in the redispatch is remunerated by the MP, incorporating efficiency losses, given that the utility had to pay for its electricity demand from the market.

Transmission reliability margin. To account for planned and unplanned line outages, we follow Weibezahn and Kendziorski [57] and apply a TRM of 25 % (effectively a reduction of the thermal line capacity, see Eqs. (17) and (18)).

Power-to-Gas and costs. In the CM model, PtG is primarily defined by the efficiency of electrolysis η_E and methanation process η_M. Based on state-of-the-art data of both components (Tables 2 and 3), we assume an efficiency of η_E = 76 % and 83 %, yielding a total PtG efficiency of 63 %. Given an average efficiency of η_e = 49 % for GfG units, electricity

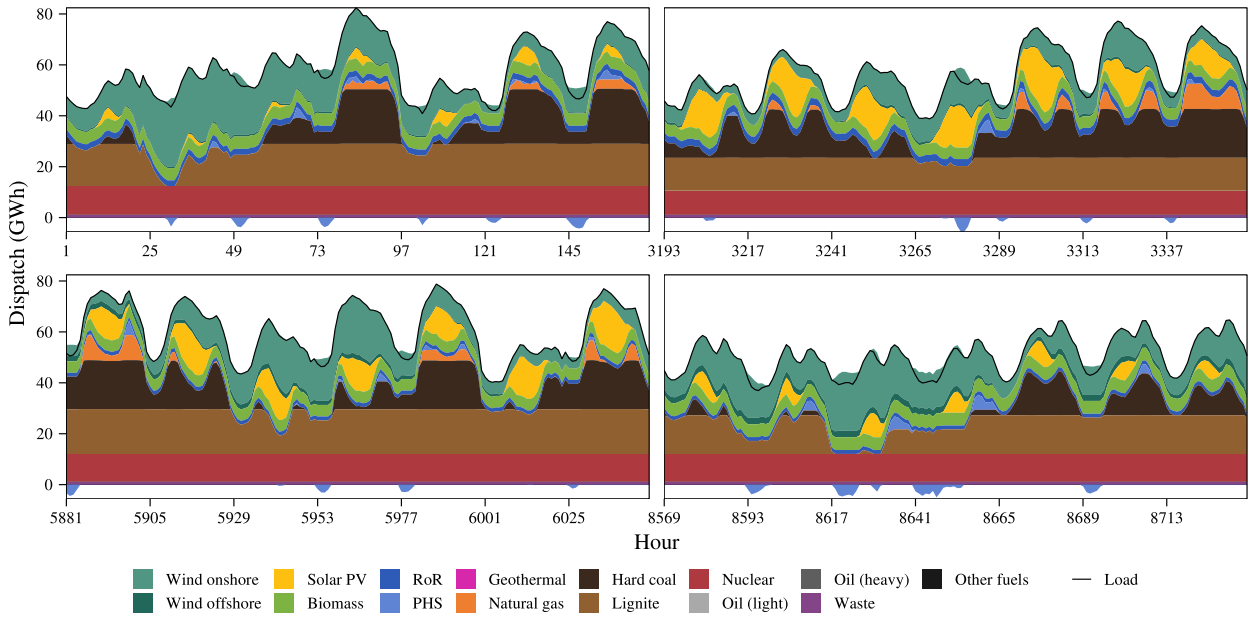

Fig. 6. Exemplary economic dispatch weeks for every quarter of the year.

generation using SNG yields a total average round-trip efficiency of 30.1 %.

Operational costs for PtG are defined by two factors, i.e., the MP and carbon neutrality. As no system-wide remuneration schemes for PtG exist to-date, we assume an indiscriminatory market, meaning that electricity demanded by PtG units is to be paid with the MP. We point out that this assumptions results in a rather conservative competitiveness of the technology. This is in parts compensated by the re-electrification of SNG through GfG units: While the MC for utilising natural gas in GfG units includes a CO_2 price per emitted ton, we assume SNG to be a carbon neutral fuel, as it is only generated from renewable wind and solar PV infeed. As such, for using SNG in GfG units, no costs for CO_2 emissions occur.

6. Model results

First, we briefly present the DA market results from the ED model, including a comparison with actual market outcomes. Second, we assess the redispatch required to account for transmission constraints with the CM model without PtG. Third, we compare how PtG as a technology for providing flexibility in redispatch affects the outcomes.

6.1. Economic dispatch

The ED determines a cost-minimal solution for meeting the total demand for each day, which sums up to 540.3 TWh over the course of a year. As a copper plate is assumed at this stage, electricity generation follows load, including demand by PHS. Fig. 6 shows four dispatch weeks at an hourly resolution. (Refer to Fig. B.20 in the Appendix B for full details including MP.) Nuclear and lignite, the most cost-efficient technologies after the intermittent RE options, both provide rather stable generation over time and operate mostly at maximum capacity. This base load follows their position in the merit order (Fig. 5). Generation by intermittent RE, solar PV and wind infeed, is more variable throughout the year. Seasonal patterns can be observed, with higher on- and offshore wind generation in winter (top left and bottom right, Fig. 6), and a higher solar PV share in summer. (top right and bottom left, Fig. 6). Since we ignore must-run obligations (which might cause RE curtailment), all RE generation is dispatched.

Demand peaks and high fluctuations in RE infeed cause GfG units to be dispatched. Further peak shaving is provided by PHS. Storing

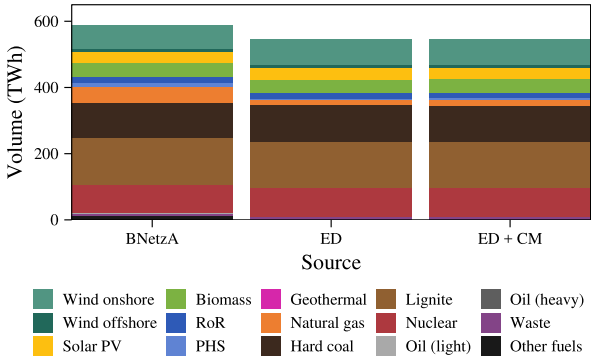

Fig. 7. Generation mix (2015). Historic data by BNetzA [60] (left), ED market results (centre), and after CM (right).

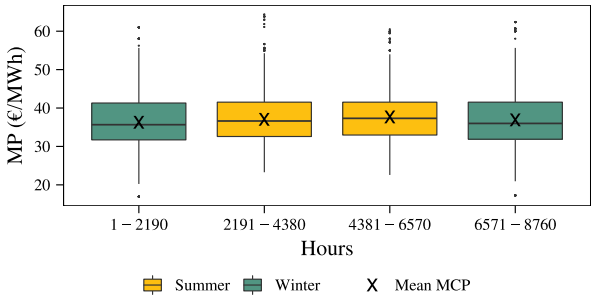

Fig. 8. Seasonal MP spread.

electricity using PHS occurs in periods with low market prices.[3] Although prices are lower in times of high RE infeed, high fluctuations in prices occur. Notably, both the average and the median price in winter

[3] The relation between prices, RE dispatch and storing can be observed in Fig. B.20 in Appendix B. Note that electricity demand by PHS is displayed on the negative Y-axis.

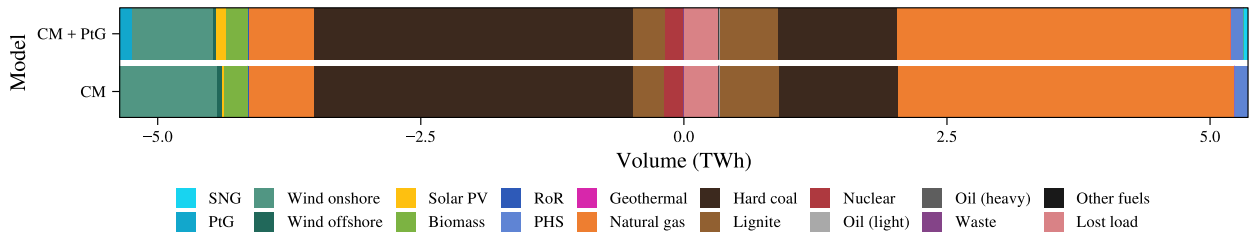

Fig. 9. Aggregated redispatch volume over a year.

(mean 36.6 €/MWh) are 2 % lower (Fig. 8) than in summer (mean 37.4 €/MWh).

High wind infeed during winter causes price fluctuations and a larger spread of the median hourly MP in winter compared to summer (31.7–41.5 €/MWh vs. 32.6–41.5 €/MWh. Fig. 8). The same figure illustrates how PHS benefit from price differences by storing when prices are low and injecting in the grid when prices are high.

Comparing model results with historic data. Comparing our results to historic data [60] gives an insight in the accuracy and validity of the model. Fig. 7 visualises the generation technology mix by BNetzA [60] (left), our ED model (centre) and after redispatch (right). It should be noted, that the BNetzA [60] data shows generation composition in retrospect, assumingly incorporating after-market corrections. As such, we primarily compare the first and last plot in Fig. 7. The height difference is due to omitting cross-border exchange from our model and is Germany's net export of about 51 TWh in 2015 [60], about 9 % of domestic demand. We obtain very similar aggregate output levels for nuclear and lignite, as well as PV and wind (both on- and offshore). Some differences in conventional technology outputs can be explained by ignoring must-run obligations. Given the high MC of GfG units, the high actual market share of 8.3 % will largely be due to must-run primarily of Combined Heat and Power (CHP) plants. Oil-based electricity generation, at less than 1 % in the real market data, is hardly ever used in our model. This most expensive option will typically only be used to deal with sudden events such as outages which are not reflected in our deterministic set up. The generation share of PHS in our model is 0.6 % only, four times lower than in [60]. This is mainly a result of limited foresight in our model, as we do not include an incentive for "left-over" PHS storage levels at the end of a day. Overall we consider the model outputs representative for the real situation in 2015 and an adequate basis for further analysis.

6.2. Congestion management and PtG utilisation

Under consideration of DC power flow transmission constraints, our CM model determines the cost-minimal redispatch of generation units across the electricity system. To respect grid constraints, that is to keep transmission flows within reliability-adjusted line capacity, the TSO makes adjustments to the ED market results. Foresee line congestion is alleviated by reducing power injection before and increasing power output behind the affected line. We present a spatial visualisation of line utilisation after CM in Fig. B.19 (in the Appendix B). The impact on the ED can especially be seen in a 0.5 percentage point higher share of GfG after redispatch (Fig. 7 right plot).

Fig. 9 displays the aggregate redispatch volume over a year; a power increase is denoted positive, a reduction or curtailment of RE negative. We include a full-year representation with daily aggregation with Fig. B.21 in Appendix B. As the market has to be balanced on a nodal level, hourly upwards and downwards adjustments are symmetric in volume.[4]

[4] Note that a total share of 3.08 % of the total redispatch volume of 10.7 TWh is attributed to lost load. 87 % of all lost load in the model is due to node 272 (Stuttgart-Weilimdorf), for which the transmission capacity of a single-circuit 220 kV line (thermal capacity of 490 MW, TRM not included) is insufficient to meet nodal load. In our case, lost load is hence mostly attributed to discrepancies between nodal load distributions assumed in the data set [58] and real life.

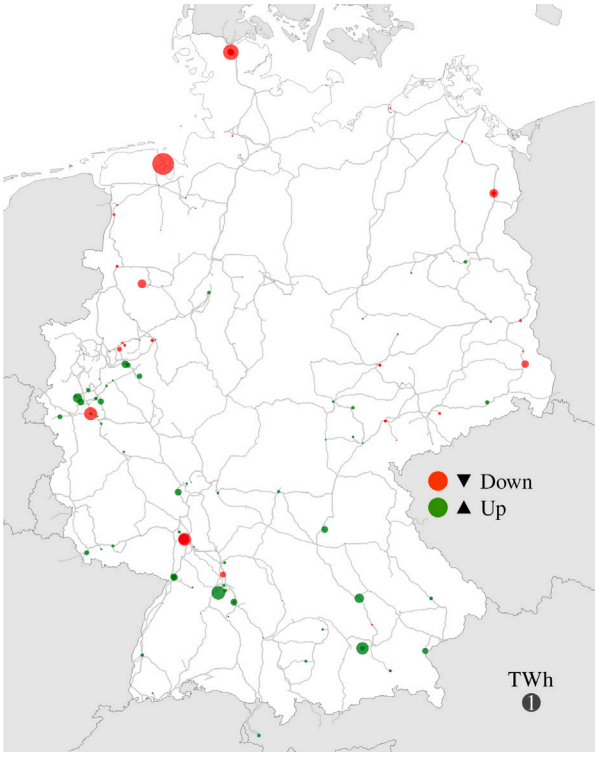

Fig. 10. Redispatch: Aggregated up- and downwards adjustments over a year.

Given the imbalanced distribution of RE, especially wind in the north, and load centres in the south, we observe a high share of wind curtailment, especially in winter. Redispatch in winter accounts for 70 % of the total annual redispatch volume. Hard coal, the cheaper option in the merit order, is dispatched in the market but reduced in the redispatch model in favour of natural gas. In times of curtailment and redispatch peaks, PHS are regulated up, accounting for 2.6 % of the total upward adjustments.

Spatial distribution of redispatch. Fig. 10 shows the spatial distribution of positive (green) and negative (red) redispatch. Negative adjustments are required mostly in the northern regions with high wind infeed. Some redispatch measures can be observed in the north east of Germany. Most upwards adjustments occur in a north to south corridor in the west of Germany.

Interestingly, the course of redispatch measures from north to south follow the planned High Voltage Direct Current (HVDC) lines (project

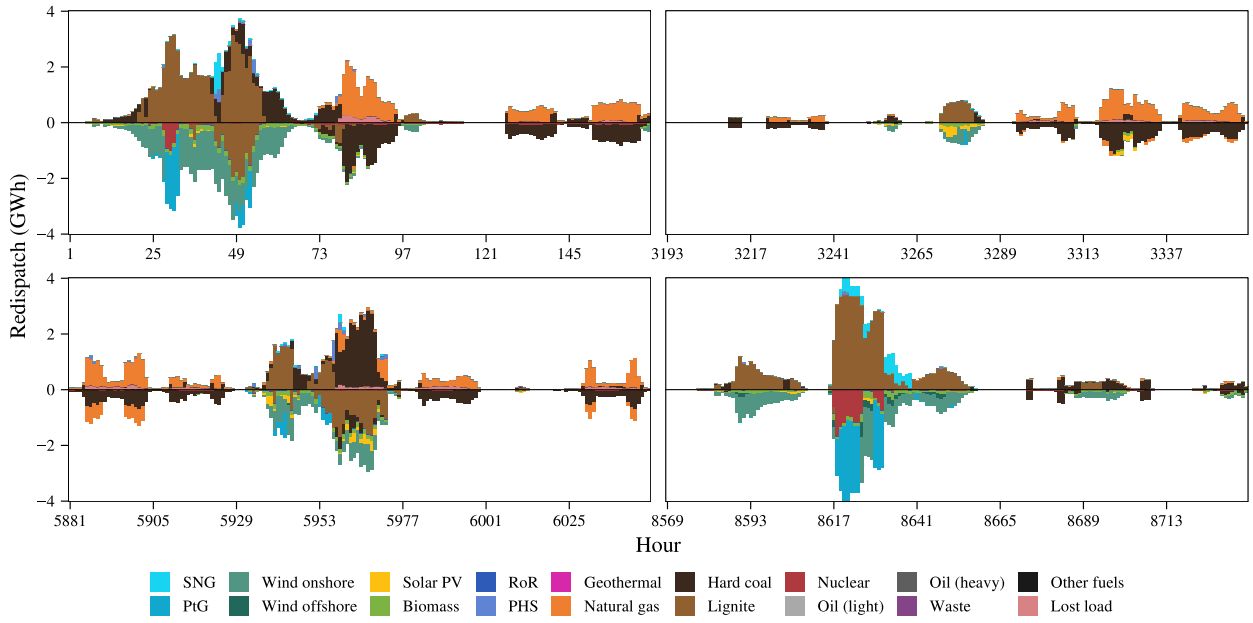

Fig. 11. Exemplary redispatch weeks including PtG for every quarter of the year.

Table 6
Top five locations for Power-to-Gas utilisation.

Substation (Node)	Lat. (°)	Long. (°)	Elec. demand (GWh_{el})
Flensburg	54.716	9.317	55.3
Bertikow	53.252	13.957	25.8
Diele	53.126	7.312	10.1
Rhede	53.026	7.254	8.0
Geithe	51.673	7.931	3.6

names "A-Nord" and "Ultranet") [6]. Both planned lines have been justified, among other reasons, by the transfer of surplus electricity from wind power parks in the North Sea [62]. Our redispatch model accounts for 69 % of the documented 15.436 TWh (redispatch) [5,63]. The difference is the result of an applied TRM of 25 % as a simplified representation of (n-1)-security, no must-run obligations, and no cross-border exchange. Omitting the first two yields less required redispatch, as (n-1) and must-run are more binding constraints than our simplification. The effect of cross-border exchange is two-fold: Depending on the temporal simultaneity and geospatial location of congested lines, it can increase or reduce the total congestion volume. Excluding the value of lost load, the total redispatch cost found by our model is 279 M€, 68 % of the documented 412 M€ [5]. This means that average per MW the redispatch cost are very close to the actual average, within 1.5 %.

Flexibility by PtG. With the addition of PtG in the CM model, the TSO is able to use the previously curtailed electricity to generate SNG. SNG can then be used as a substitute for natural gas in the upwards generation of redispatch, shifting energy from the north to the south without increasing pressure on the electricity grid. This alternative is attractive at a sufficiently low MP, often the case in times of high RE infeed. Therefore, SNG is produced especially in winter time, when both wind availability and curtailment are high. Fig. 11 illustrates this behaviour.

The results show that in 173 h of the year, it is attractive to use PtG; more than 80 % of PtG usage occurs during the winter. In 379 h, SNG partially replaces natural gas in GfG units. Effectively, this leads to a total reduction in RE curtailment (negative redispatch) by 12.1 % and a substitution of natural gas for positive redispatch by 1.2 % (Fig. 9).

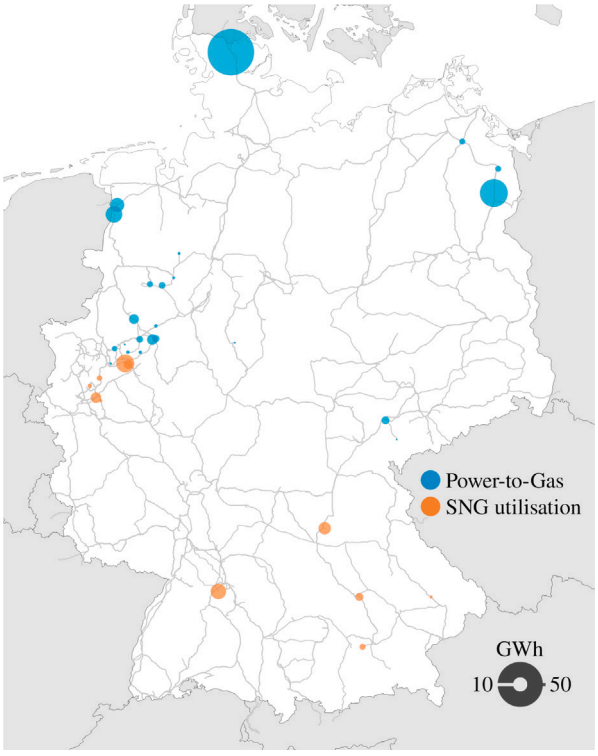

Fig. 12. Power-to-Gas and SNG utilisation in redispatch over a year.

Location of PtG units. In Fig. 12 we display all nodes where PtG is utilised and SNG re-electrified through GfG units. As the production of SNG is directly related to the volume of wind curtailment, the locations match nodes with high wind availability and redispatch volumes.

We list the top five locations of PtG utilisation for providing flexibility in Table 6. Similarly, SNG is used in location where positive redispatch through GfG is most cost-effective to mitigate line congestion. Notably, these results reflect the locations of two PtG projects. The

Table 7
Parameter variations in sensitivity runs: Electrolysis efficiency η_E, methanation efficiency η_M, and total efficiency η.

η_E	.72	.74	.76	.76	.76	.76	.76
η_M	.83	.83	.83	.84	.86	.88	.90
η	.60	.61	.63	.64	.65	.67	.68

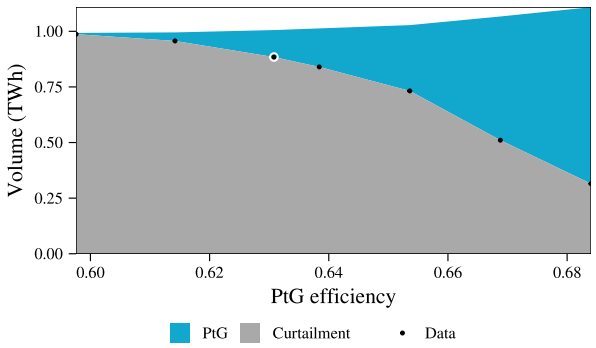

Fig. 13. Sensitivity of PtG utilisation and RE curtailment in total volume. Data points represent individual sensitivity runs.

first is "hybridge" [64], a 100 MW electrolyser to be installed in Lingen, close to the Dutch border. It is a joint project by one of the German electricity TSO Amprion in cooperation with the gas TSO Open Grid Europe. The second is a cooperation between the German electricity TSO TenneT, gas TSOs Gasunie and Thyssengas at the estuary of the river Ems, connected to the substation in Diele (Table 6). "ElementEins" consists of a 100 MW electrolyser too, and primarily aims at utilising offshore and onshore wind electricity [65]. Given their good connection to natural gas storages and access to biogenic CO_2, both projects are planned with methanation units. Furthermore, the locations found also overlap with optimal locations for PtG units determined by Haumaier et al. [36]. This indicates that these locations are not only of interest from a transmission-supporting, but also from an economic point of view for future PtG operators.

7. Sensitivity analysis

This section is dedicated to gaining deeper insight in how the model results react to changes in input parameters, specifically PtG efficiency, RE infeed, and changes in CO2 prices.

7.1. Varying PtG efficiencies

In the original data set the efficiency for electrolysis rate was set at 76 %, and 83 % for methanation. As presented in Section 1, efficiencies vary depending on different factors and underlying technologies. One of the main factors we have found is the utilisation of heat. Since the methanation process is an exothermic reaction, high quality steam is produced as byproduct. By using this waste heat, a higher efficiency for methanation can be achieved, resulting in an increase of system efficiencies [66]. The efficiency for PEM electrolysis used above is the high end of the range when not considering waste heat utilisation.

Based on the PtG technology and project overview (Tables 1–3) we run sensitivities with decreased electrolysis and increased methanation efficiencies (Table 7). This analysis shows that the potential of PtG is in fact highly sensitive to changes in efficiency. Figs. 13 and 14 display the relation between a marginal change in total PtG efficiency (denoted on the vertical axis) to the volume of PtG utilisation and RE curtailment based on the total volume and hours over the year, respectively.

As the costs for PtG are directly determined through the MP and efficiency losses (Eq. (23)), an efficiency increase directly translates into a higher competitiveness of the technology. A total PtG efficiency

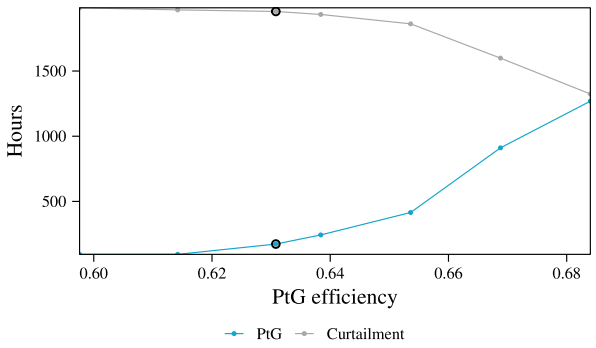

Fig. 14. Sensitivity of PtG utilisation and RE curtailment in total hours.

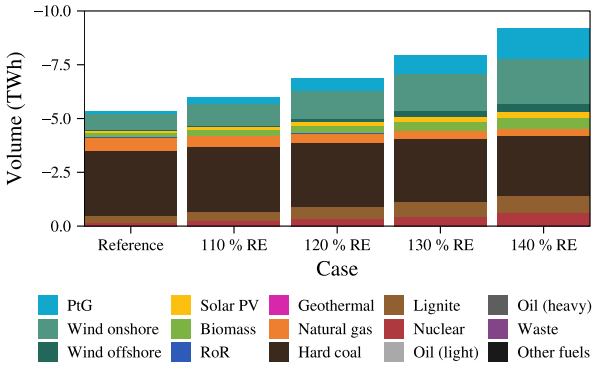

Fig. 15. Downwards adjustments in redispatch for increasing RE shares.

of around 65 % already leads to PtG utilisation in 415 h of the year, which corresponds to more than two-times the utilisation of our reference case. With a methanation efficiency of $\eta_M = 0.90$, PtG is used in 1269 h, decreasing curtailment measures in 1957 h down to 1324 h. Accordingly, the demanded electricity by PtG for SNG production sees a rise from 173 GWh to 793 GWh, reducing overall curtailment volume by 64 % in comparison to our reference. On the other hand, a total PtG efficiency below 61 %, makes PtG effectively non-competitive, given the MP structure of our model over the year.[5]

7.2. Increasing the share of RES

Given the foreseen future additions of RE capacities [6], we investigate how our model results react to an increase in RE shares. Specifically, we vary installed capacities of intermittent RE, i.e., solar PV, wind offshore, and onshore. In four separate model runs, we increase the installed capacities of intermittent RE at every node by 10 up to 40 %. The maximum generation of RE sources follows the same availability time series from our original data set.

Naturally, a growth of intermittent RE capacities will proportionally result in increased generation by solar PV and wind in the ED. As such, curtailment of RE will increase more than proportional to higher installed RE capacities.

In Fig. 15, we see an increase of intermittent RE by 10 % translating to close to doubling of PtG utilisation.

While in our reference case PtG utilisation lies at 121.3 GWh, we see an almost twelve-fold increase to 1415 GWh for a 40 % increase of installed intermittent RE capacities. Two main reasons are that more curtailed renewable electricity is available, and that more RE in the day-ahead spot market (ED) pushes all conventional power plants in the merit order to the right, resulting in a lower MP. Fig. 16 shows

[5] See Fig. B.20 in Appendix B.

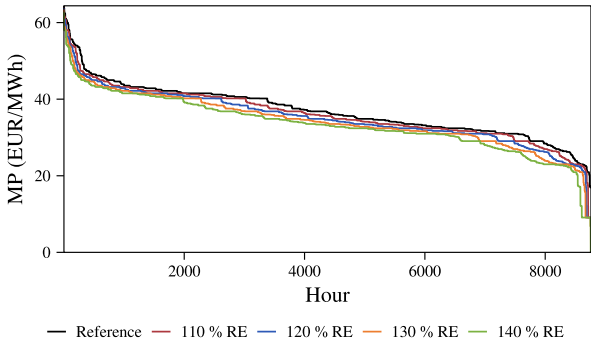

Fig. 16. Market clearing price duration curve for increasing RE shares.

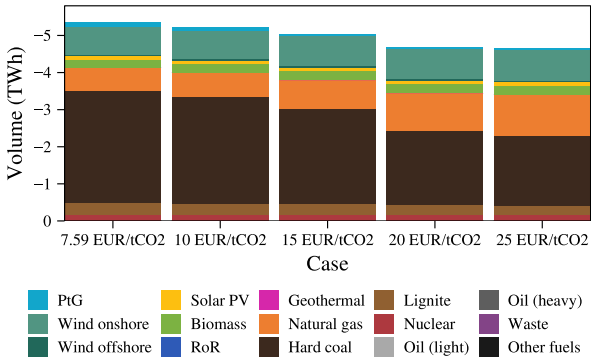

Fig. 17. Downwards adjustments in redispatch for increasing CO_2 prices.

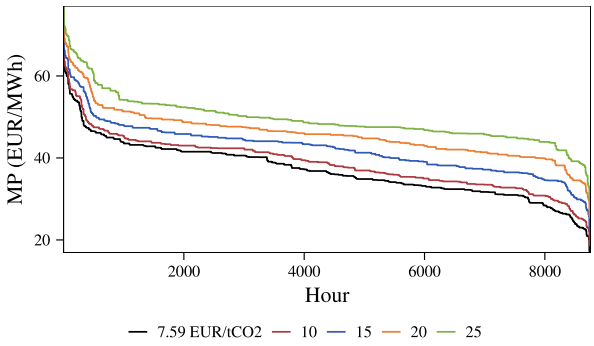

Fig. 18. Market clearing price duration curve for increasing CO_2 prices.

the duration curve of the MP for the model year. The MP decreases by about 2 to 2.5 % from one sensitivity case to the next (for each 10 percent increase in RE capacity).

As for the downwards adjustment of conventional power plants, there are multiple effects to be observed (Fig. 15): Negative changes to hard coal based electricity generation remain very stable at 2.8 to 3.0 TWh. Negative redispatch of GfG units decreases from 621 GWh (reference) to 336 GWh (140 % RE). As for nuclear and lignite power plants, downwards adjustments grow from 178 GWh and 303 GWh (reference) to 626 GWh and 769 GWh (140 % RE), respectively. The explanation for the two counteracting developments is as follows: Based on the merit order in Fig. 5, the average load in the German electricity is covered by hard coal as the marginal generating technology. Following our above explanation, more expensive fuels such as natural gas have been crowded out from the market, already. As such, with an increase in RE and less natural gas based electricity in the dispatch, the CM model receives a lower natural gas volume that can be reduced through negative redispatch. The opposite can be said for both nuclear and lignite, being left of hard coal in the merit order.

7.3. Changing the CO_2 price

In 2015, every emitted tonne of CO_2 was priced at only 7.59 €/MWh on average [56]. However, developments in recent years show a surge in CO_2 emission costs.[6] As such, we investigate how a higher CO_2 price affects the potential of PtG.

At a CO_2 price of 10 € per emitted tonne, PtG utilisation has already decreased by 15 %. A CO_2 price of 25 €/tCO_2 pushes PtG utilisation down to 35 GWh. While counter-intuitive at first, there is a logical explanation for this behaviour, that is the dynamic interaction between (i) the ED and CM model and (ii) the direct dependency of costs for PtG on the MP.

(I) With the lowest emission factor of only 0.49 tCO_2 per MWh_{th}, natural gas has a 47 % lower emission rate then its neighbouring fuel in the merit order, hard coal. As such, natural gas as a generation technology is affected much less by an increase in CO_2 price relative to all other conventional technologies. As such, now being a much cheaper option, natural gas is in parts substituting the dispatch of hard coal. From the perspective of the CM model, this leads to less hard coal and more natural gas being downward adjusted (Fig. 17). In addition we observe an overall reduction in required redispatch volume with a lower share of hard coal based electricity generation in the economic dispatch (Fig. 17). From the change 20 to 25 €/tCO_2 price, the reduction in total downwards adjustments remains close to unchanged. Given the more beneficial locations of natural gas power plants after frequently congested lines in the German electricity system compared to hard coal (cf. Figs. B.19 and B.23), total redispatch volume decreases. The two last columns in Fig. 17 can hence be seen as the "minimum" in required downward adjustments given the German grid topology of 2015.

(II) Not only in comparison to all other fossil fuels, natural gas based electricity is now much more competitive, but also compared to SNG based electricity. This is due to the fact, that one of our key assumptions in the model is an indiscriminatory market. To utilise PtG to produce SNG, electricity has to be paid for at the MP. In Fig. 18, we can see that an increase in CO_2 costs effectively shifts the average MP proportionally. Given the total average round-trip efficiency by SNG based electricity of 30.1 % (including the thermal efficiency of GfG units), PtG now becomes a very cost-intensive technology. These increases in costs are not compensated by the mitigation of CO_2 costs when using SNG for generating electricity in GfG units.

We point out that this sensitivity does not mean that PtG is an infeasible or uneconomical technology given a higher CO_2 price. With an increasing share of RE in the future, both the volume of RE and a higher CO_2 price can push fossil fuel based generation entirely out of the merit order. This again would result in a larger price spread, making PtG attractive again. What we take from this analysis however is the fact that given our underlying assumption of an indiscriminatory market, PtG utilisation is highly sensitive to the remuneration mechanisms and MP in place.

8. Conclusion

In this paper, we have assessed the potential of PtG in combination with GfG units providing flexibility specifically to support redispatch measures, given the geographical mismatch of load and RE infeed as

[6] A real-time development of CO_2 emission allowance price can be found in https://markets.businessinsider.com/commodities/co2-european-emission-allowances.

well as limited transmission capacities. We have argued, that the need for flexibility increases not only with the variability and fluctuation of RE, but also because of spatial imbalances between generation and demand. Through the utilisation of PtG at nodes facing high RE curtailment, we add flexibility to the system both on a spatial and temporal level. Through sector coupling, a higher level of RE injection into the generation mix at lower or equal stress on congested transmission lines can be achieved.

We illustrate that a few bottlenecks in the transmission grid are responsible for most of the curtailment. These locations are primarily characterised by high wind infeed, especially in the winter season. In order to meet demand in the south, GfG units provide positive redispatch. With the long-term goal of transitioning to a low carbon or zero-carbon energy system, the curtailment of RE and upwards adjustment of conventional, carbon-intense power plants is counterproductive, unecological and cost-intensive. By implementing PtG, otherwise curtailed electricity from the north has been shifted towards load centres in the south of Germany, making use of existing gas infrastructures.

The results also give an indication of attractive PtG locations in the transmission grid that lack flexibility, i.e., nodes with large amounts of curtailed RE. Instead of curtailing RE sources, we are able to utilise RE in a reasonable way. Unlike PHS or battery-based storages, the combination of PtG and SNG utilisation is not bound to a single location. Given the well-developed, meshed gas infrastructure in Germany, it allows for injecting to and extracting from different locations. We point out that the attractiveness and competitiveness of PtG depends on investment cost and additional applications outside of congestion management. For example, synergies with other technologies and sectors, such as the heat and transportation sector should be investigated in future research. To a certain share of the total gas volume, a direct injection of hydrogen into the gas grid may be possible. This would circumvent the methanation process and improve both energy and cost efficiency, significantly.

Given the price sensitivity of the model, representing must-run obligations in our model may impact the assessed potential of PtG. If must-run capacity were to be implemented, the underlying data have to be robust to yield reliable model results. Similarly, the potential for PtG increase with higher RE shares and longer periods with low electricity prices. In addition, further research may as well include a European perspective, including the modelling of cross-border trade and countertrading. Possibly, this will result in both increases as well as alleviations of inland congestion in certain hours. We point out that our sensitivity analysis based on marginal efficiency changes of PtG is equivalent to varying the MP, e.g. as a result of future changes in fuel prices, incorporation of must-run, or cross-border exchange.

Apart from a technical and economical point of view, an analysis of the regulatory framework should also be part of further research. Grid infrastructures are natural monopolies and TSOs in liberalised energy markets are regulated entities. As such, adaptations of current frameworks with regards to utilisation of PtG by TSOs, e.g. as transmission assets, may be necessary. The results in our paper show that PtG deserves attention as a potential flexibility provider in future low carbon energy systems with high shares of renewables.

Acronyms

AC Alternating Current.

AEL Alkaline Water Electrolysis.

BNetzA Bundesnetzagentur (Federal Network Agency).

CHP Combined Heat and Power.

CM Congestion Management.

DA Day-Ahead.

DC Direct Current.

ED Economic Dispatch.

GfG Gas-fired Generation.

HVDC High Voltage Direct Current.

JuMP Julia for Mathematical Programming.

LP Linear Program.

MC Marginal Cost.

MP Market Clearing Price.

O&M Operation and Maintenance.

PEM Polymer Electrolyte Membrane.

PHS Pumped Hydroelectric Storage.

PtG Power-to-Gas.

PV Photovoltaics.

RE Renewable Energy.

RoR Hydro Run-of-River.

SNG Synthetic Natural Gas.

SOEC Solid Oxide Electrolyte Electrolysis.

TRM Transmission Reliability Margin.

TSO Transmission System Operator.

CRediT authorship contribution statement

Bobby Xiong: Coding and modelling effort, Data research and writing the paper, Reviewing and editing. **Johannes Predel:** Coding and modelling effort, Data research and writing the paper, Reviewing and editing. **Pedro Crespo del Granado:** Paper concept and scope development, supervised the model formulation, implementation, reviewing and editing. **Ruud Egging-Bratseth:** Supervised the model formulation, Implementation, Reviewing and editing.

Declaration of competing interest

The authors declare that they have no known competing financial interests or personal relationships that could have appeared to influence the work reported in this paper.

Acknowledgements

A special acknowledgement to the openENTRANCE project in which several case studies analyse the need of flexibility in a decarbonised energy system. The openENTRANCE project has received funding from the European Union's Horizon 2020 programme (grant No. 835896).

Model framework

We provide our model (Julia) and visualisation framework (R) under the MIT licence on GitHub: github.com/bobbyxiong/redispatch-ptg.

Appendix A. Model terminology

Sets. Sets are denoted by scripted, uppercase letters and contain a finite number of indices used in the mathematical model.

$\mathcal{N}$	Set of nodes: n, m
$\mathcal{G}$	Set of all power plants: g
$\mathcal{R}$	Subset of $\mathcal{G}$, RE units: r
$\mathcal{E}$	Subset of $\mathcal{G}$, GfG units: e
$\mathcal{S}$	Set of PHS: s
$\mathcal{L}$	Set of transmission lines: $l \in (n, m)$
$\mathcal{T}$	Set of time slices in hours: t

Variables. Variables are represented by uppercase letters and are endogenously optimised by the model. They can span over multiple sets.

Ψ_t	MP in €/MWh$_{el}$
$P^{DA}_{g,t}$	Generated power on the spot market (day-ahead) in MW$_{el}$
$P^{DA}_{s,t}$	Generated power from PHS on the spot market (day-ahead) in MW$_{el}$
$P^{inj}_{n,t}$	Power injection at node n in MW$_{el}$
$\Delta P^{+}_{g,t}$	Upwards adjustment of the spot market generation in MW$_{el}$
$\Delta P^{-}_{g,t}$	Downwards adjustment of the spot market generation in MW$_{el}$
$\Delta P^{+}_{s,t}$	Upwards adjustment of the spot market generation from PHS in MW$_{el}$
$P^{lost}_{n,t}$	Lost load at node n in MW$_{el}$
$P^{flow}_{n,m,t}$	Line flow from n to m in MW$_{el}$
$\Theta_{n,t}$	Voltage angle at node n and m in rad
$P^{PtG}_{e,t}$	Generated power using SNG in MW$_{el}$
$D_{s,t}$	Demand of PHS unit in MW$_{el}$
$D^{PtG}_{r,t}$	Demand of PtG facility in at the location of r in MW$_{el}$
$L_{s,t}$	Storage level of PHS unit in MWh$_{el}$
L_t	Virtual SNG storage level in MWh$_{th}$

Parameters. Parameters are denoted by lowercase letters and are exogenously determined by input data. Their dimension can span over multiple sets. To link the two model parts and transfer the model output of the first parts to the second, we use *auxiliary parameters*. Results for variables in the DA model that are used as fixed input (parameters) for the CM model are depicted with an overline.

$b_{n,m}$	Susceptance entry (n, m)
c^{mc}_{g}	Marginal cost of power plant in €/MWh$_{el}$
$c^{mc,PtG}_{g}$	Marginal cost of power plant in €/MWh$_{el}$ using SNG
c^{fuel}	Fuel cost in €/MWh$_{el}$
c^{OM}_{g}	Operation and maintenance cost in €/MWh$_{el}$
c^{CO_2}	CO_2 price in €/tCO_2
c^{VOLL}	Value of lost load in €/MWh$_{el}$
$d^{load}_{n,t}$	Load in MW$_{el}$
d^{max}_{r}	Maximum PtG output/electricity demand in MW$_{el}$
η_g	Efficiency of power plant in MW$_{el}$/MW$_{th}$
η_s	Pumping efficiency of PHS unit
η_E	Efficiency factor of electrolysis in MW$_{th}$/MW$_{el}$
η_M	Efficiency factor of methanation in MW$_{th}$/MW$_{th}$
l^{init}	Initial storage level of the virtual SNG storage in MWh$_{th}$
λ_g	CO_2 factor of power plant in tCO_2/MWh$_{th}$
p^{max}_{g}	Maximum power generation limit in MW$_{el}$
p^{min}_{g}	Minimum power generation limit in MW$_{el}$
p^{rup}_{g}	Ramp up rate in MW$_{el}$/h
p^{rdn}_{g}	Ramp down rate in MW$_{el}$/h
p^{max}_{s}	Maximum power generation and pumping limit of a PHS unit in MW$_{el}$
p^{max}_{l}	Line capacity in MW$_{el}$
x_l	Line reactance in MW$_{el}$
l^{max}_{s}	Storage capacity of PHS unit in MWh$_{el}$
trm	TRM between 0 and 1

Appendix B. Material

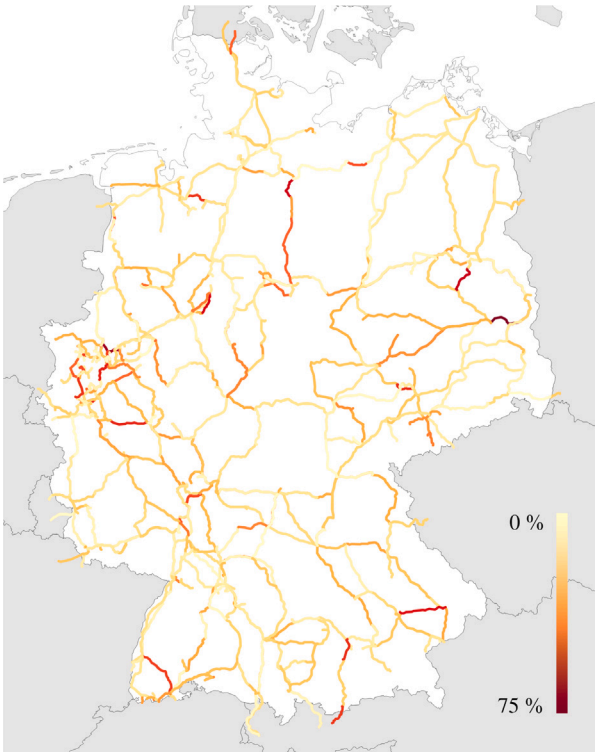

Fig. B.19. Average transmission line utilisation after CM.

Table B.8
Case study — Fuel costs, variable O&M costs, and emission factors based on Kunz et al. [58].

Technology	Avg. power plant efficiency η_g (%)	Fuel costs c^{fuel} (€/MWh$_{th}$)	Var. O&M costs c_g^{OM} (€/MWh$_{el}$)	Avg. emission factor λ_g (tCO$_2$/MWh$_{th}$)
Nuclear	33.0	3.00	0	0
Lignite	37.5	6.22	0	0.98
Hard coal	40.2	10.61	0.53 – 6.53	0.86
Natural gas	42.6	22.76	0	0.49
Oil (heavy)	37.5	22.04	0	0.78
Oil (light)	34.5	45.74	0	0.78
Waste	33.2	0	0	0
Other fuels	33.3	45.74	0	0

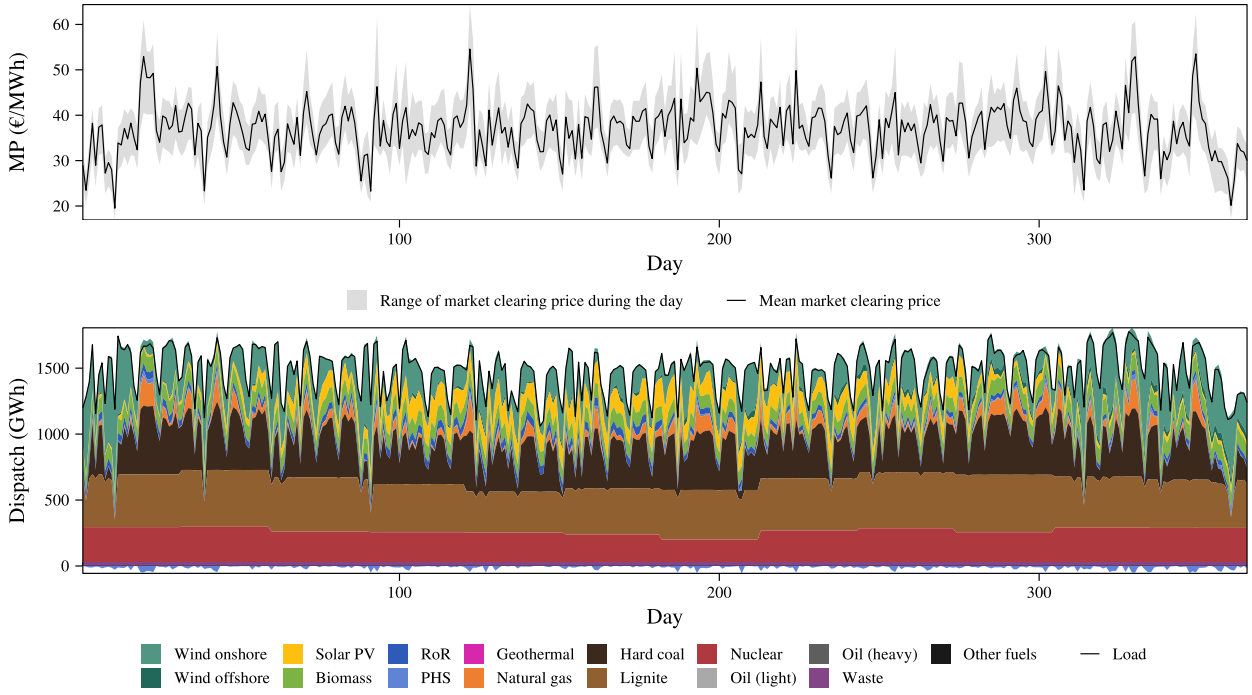

Fig. B.20. Daily ED and MP range. Note that the dispatch is summed up over the day.

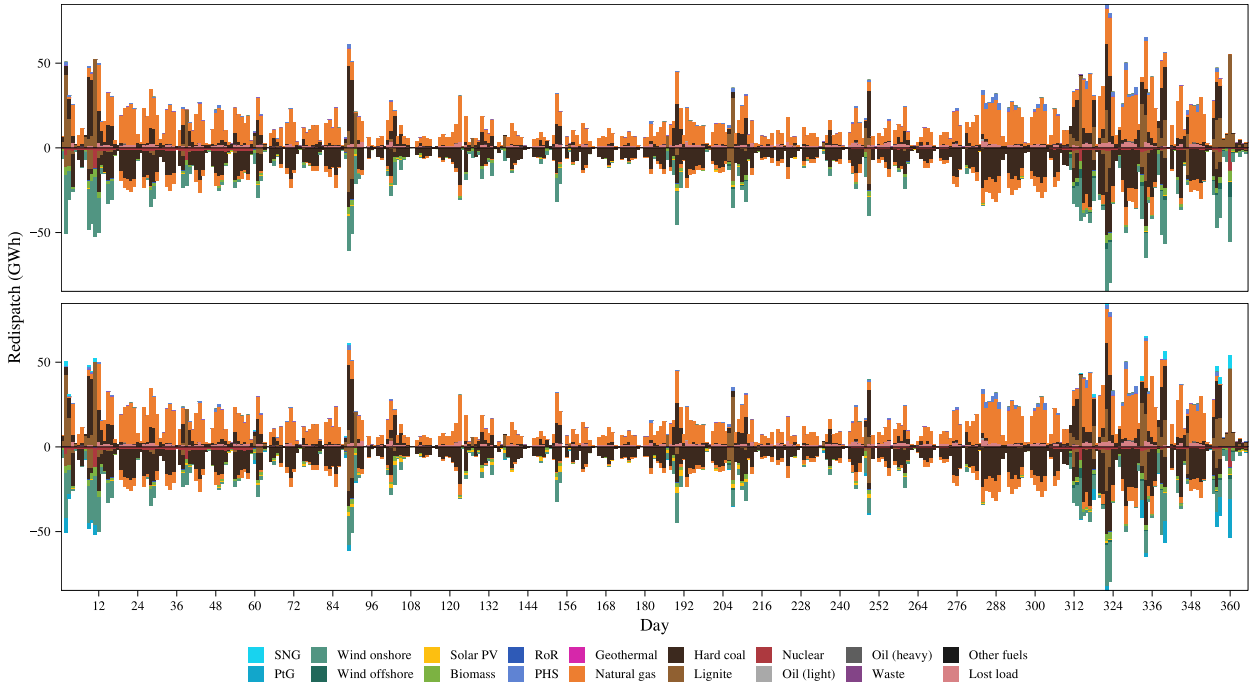

Fig. B.21. Daily CM redispatch volume (top) and including PtG (bottom).

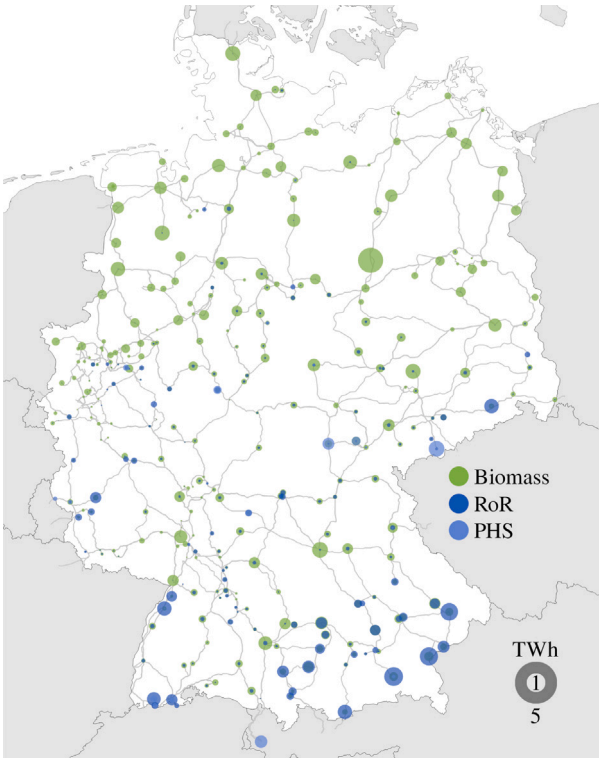

Fig. B.22. Electricity generation by flexible RE sources over a year.

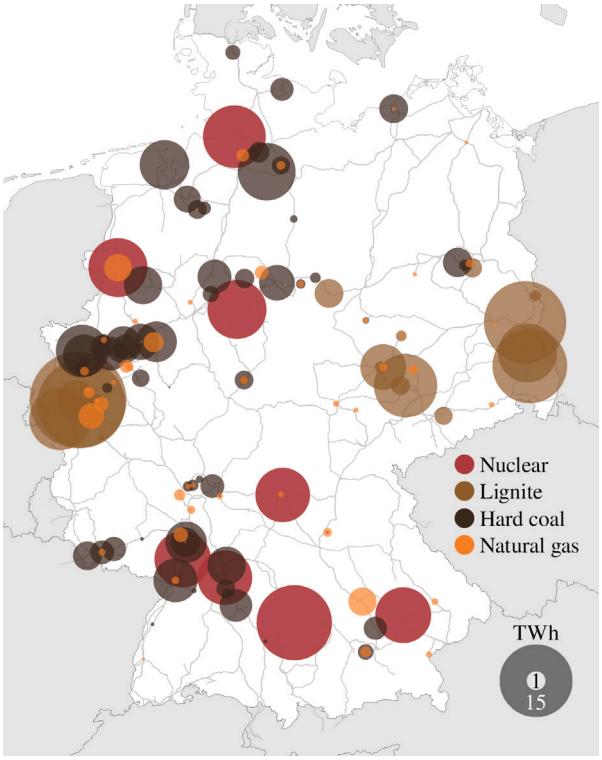

Fig. B.23. Electricity generation by conventional power plants over a year.

References

[40] Zapf M. Stromspeicher und power-to-gas im deutschen energiesystem. Wiesbaden: Springer Fachmedien Wiesbaden; 2017, http://dx.doi.org/10.1007/978-3-658-15073-0, URL: http://link.springer.com/10.1007/978-3-658-15073-0.

[66] Younas M, Loong Kong L, Bashir MJK, Nadeem H, Shehzad A, Sethupathi S. Recent advancements, fundamental challenges, and opportunities in catalytic methanation of CO $_2$$. Energy Fuels 2016;30(11):8815–31. http://dx.doi.org/10.1021/acs.energyfuels.6b01723, URL: https://pubs.acs.org/doi/10.1021/acs.energyfuels.6b01723.

[1] BNetzA, BNetzA. 3. Quartalsbericht 2015 zu netz- und systemsicherheitsmaßnahmen: Viertes quartal 2015 sowie gesamtjahresbetrachtung 2015. Bericht, Bonn, Germany: Bundesnetzagentur; 2016, URL: https://www.bundesnetzagentur.de/SharedDocs/Downloads/DE/Allgemeines/Bundesnetzagentur/Publikationen/Berichte/2016/Quartalsbericht_Q4_2015.pdf.

[2] BNetzA, BNetzA. Quartalsbericht zu netz- und systemsicherheitsmaßnahmen: Viertes quartal und gesamtjahr 2016. Bericht, Bonn, Germany: Bundesnetzagentur; 2017, URL: https://www.bundesnetzagentur.de/SharedDocs/Downloads/DE/Allgemeines/Bundesnetzagentur/Publikationen/Berichte/2017/Quartalsbericht_Q4_Gesamt_2016.pdf.

[3] BNetzA, BNetzA. Quartalsbericht zu netz- und systemsicherheitsmaßnahmen: Gesamtjahr und viertes quartal 2017. Bericht, Bonn, Germany: Bundesnetzagentur; 2018, URL: https://www.bundesnetzagentur.de/SharedDocs/Downloads/DE/Allgemeines/Bundesnetzagentur/Publikationen/Berichte/2018/Quartalsbericht_Q4_Gesamt_2017.pdf.

[4] BNetzA, BNetzA. Quartalsbericht zu netz- und systemsicherheitsmaßnahmen: Gesamtjahr und viertes quartal 2018. Bericht, Bonn, Germany: Bundesnetzagentur; 2019, URL: https://www.bundesnetzagentur.de/SharedDocs/Downloads/DE/Allgemeines/Bundesnetzagentur/Publikationen/Berichte/2019/Quartalsbericht_Q4_2018.pdf.

[5] BNetzA, BNetzA. Quartalsbericht netz- und systemsicherheit - gesamtes jahr 2019. Bericht, Bonn, Germany: Bundesnetzagentur; 2020, URL: https://www.bundesnetzagentur.de/SharedDocs/Mediathek/Berichte/2020/Quartalszahlen_Gesamtjahr_2019.pdf.

[6] 50Hertz, Amprion, TenneT, TransnetBW, 2019. Netzentwicklungsplan Strom 2030, Version 2019: Zweiter Entwurf der Übertragungsnetzbetreiber. Technical Report. Germany. URL: https://www.netzentwicklungsplan.de/.

[7] Heggarty T, Bourmaud J-Y, Girard R, Kariniotakis G. Multi-temporal assessment of power system flexibility requirement. Appl Energy 2019;238:1327–36. http://dx.doi.org/10.1016/j.apenergy.2019.01.198, URL: https://linkinghub.elsevier.com/retrieve/pii/S0306261919302107.

[8] Huber M, Dimkova D, Hamacher T. Integration of wind and solar power in Europe: Assessment of flexibility requirements. Energy 2014;69:236–46. http://dx.doi.org/10.1016/j.energy.2014.02.109, URL: https://linkinghub.elsevier.com/retrieve/pii/S0360544214002680.

[9] Ma J, Silva V, Belhomme R, Kirschen DS, Ochoa LF. Exploring the use of flexibility indices in low carbon power systems. In: 2012 3rd IEEE PES innovative smart grid technologies Europe (ISGT Europe). Berlin, Germany: IEEE; 2012, p. 1–5. http://dx.doi.org/10.1109/ISGTEurope.2012.6465757, URL: http://ieeexplore.ieee.org/document/6465757/.

[10] Rosen C. An option-based approach for the fair pricing of flexible electricity supply. SSRN Electron J 2015. http://dx.doi.org/10.2139/ssrn.2831340, URL: http://www.ssrn.com/abstract=2831340.

[11] Perera A, Nik VM, Wickramasinghe P, Scartezzini J-L. Redefining energy system flexibility for distributed energy system design. Appl Energy 2019;253:113572. http://dx.doi.org/10.1016/j.apenergy.2019.113572, URL: https://linkinghub.elsevier.com/retrieve/pii/S0306261919312462.

[12] Müsgens F, Ockenfels A, Peek M. Economics and design of balancing power markets in Germany. Int J Electr Power Energy Syst 2014;55:392–401. http://dx.doi.org/10.1016/j.ijepes.2013.09.020, URL: https://linkinghub.elsevier.com/retrieve/pii/S014206151300402X.

[13] Kondziella H, Bruckner T. Flexibility requirements of renewable energy based electricity systems – a review of research results and methodologies. Renew Sustain Energy Rev 2016;53:10–22. http://dx.doi.org/10.1016/j.rser.2015.07.199, URL: https://linkinghub.elsevier.com/retrieve/pii/S1364032115008643.

[14] Schill W-P. Residual load, renewable surplus generation and storage requirements in Germany. Energy Policy 2014;73:65–79. http://dx.doi.org/10.1016/j.enpol.2014.05.032, URL: https://linkinghub.elsevier.com/retrieve/pii/S0301421514003310.

[15] Castagneto Gissey G, Subkhankulova D, Dodds PE, Barrett M. Value of energy storage aggregation to the electricity system. Energy Policy 2019;128:685–96. http://dx.doi.org/10.1016/j.enpol.2019.01.037, URL: https://linkinghub.elsevier.com/retrieve/pii/S0301421519300655.

[16] Østergaard PA. Comparing electricity, heat and biogas storages' impacts on renewable energy integration. Energy 2012;37(1):255–62. http://dx.doi.org/10.1016/j.energy.2011.11.039, URL: https://linkinghub.elsevier.com/retrieve/pii/S0360544211007705.

[17] Allard S, Mima S, Debusschere V, Quoc TT, Criqui P, Hadjsaid N. European transmission grid expansion as a flexibility option in a scenario of large scale variable renewable energies integration. Energy Econ 2020;87:104733. http://dx.doi.org/10.1016/j.eneco.2020.104733, URL: https://linkinghub.elsevier.com/retrieve/pii/S0140988320300724.

[18] Nabe C, Neuhoff K. Intraday- and real time activity of TSOs: Germany. DIW - Deutsches Institut für Wirtschaftsforschung; 2015, URL: http://hdl.handle.net/10419/111265.

[19] Connect. Konzepte für redispatchbeschaffung und bewertungskriterien. 2018, URL: https://www.bmwi.de/Redaktion/DE/Publikationen/Studien/konzepte-fuer-redispatch.pdf?_blob=publicationFile&v=6.

[20] dena, dena. Wechselwirkungen zwischen regelleistungserbringung und netzengpässen im verteilnetz. 2017.

[21] Hadush SY, Meeus L. DSO-TSO cooperation issues and solutions for distribution grid congestion management. Energy Policy 2018;120:610–21. http://dx.doi.org/10.1016/j.enpol.2018.05.065, URL: https://linkinghub.elsevier.com/retrieve/pii/S0301421518303823.

[22] dena, dena. Strategieplattform power-to-gas: Projektkarte. 2020, URL: https://www.powertogas.info/projektkarte/.

[23] StoreandGo, StoreandGo. The German demonstration site at falkenhagen. 2019, URL: https://www.storeandgo.info/demonstration-sites/germany/.

[24] Aryal N, Kvist T, Ammam F, Pant D, Ottosen LD. An overview of microbial biogas enrichment. Bioresour Technol 2018;264:359–69. http://dx.doi.org/10.1016/j.biortech.2018.06.013, URL: https://linkinghub.elsevier.com/retrieve/pii/S0960852418307922.

[25] Heidrich T, Filzek D, Ritter P. Endbericht: BioPower2Gas - vergleichende simulation, demonstration und evaluation von optimal leistungsregelbaren biogastechnologien. 2017, URL: https://www.house-of-energy.org/mm/03KB089_Endbericht_BioPower2Gas.pdf.

[26] Ghaib K, Ben-Fares F-Z. Power-to-Methane: A state-of-the-art review. Renew Sustain Energy Rev 2018;81:433–46. http://dx.doi.org/10.1016/j.rser.2017.08.004, URL: https://linkinghub.elsevier.com/retrieve/pii/S1364032117311346.

[27] Gruber M, Weinbrecht P, Biffar L, Harth S, Trimis D, Brabandt J, Posdziech O, Blumentritt R. Power-to-Gas through thermal integration of high-temperature steam electrolysis and carbon dioxide methanation - Experimental results. Fuel Process Technol 2018;181:61–74. http://dx.doi.org/10.1016/j.fuproc.2018.09.003, URL: https://linkinghub.elsevier.com/retrieve/pii/S037838201831155X.

[28] Zuberbuehler U. Verbundprojekt power-to-gas: Errichtung und betrieb einer forschungsanlage zur speicherung von erneuerbarem strom als erneuerbares methan im 260kw maßstab. Technical Report, Techn. Informationsbibl. und Univ.-Bibl.; 2014, URL: https://www.tib.eu/suchen/id/TIBKAT:844211427/.

[29] Kloubert M-L, Schwippe J, Muller SC, Rehtanz C. Analyzing the impact of forecasting errors on redispatch and control reserve activation in congested transmission networks. In: 2015 IEEE eindhoven powertech. Eindhoven, Netherlands: IEEE; 2015, p. 1–6. http://dx.doi.org/10.1109/PTC.2015.7232716, URL: http://ieeexplore.ieee.org/document/7232716/.

[30] Consentec. Quantitative analysen zu beschaffungskonzepten für redispatch. 2019, URL: https://www.bmwi.de/Redaktion/DE/Publikationen/Studien/untersuchung-zur-beschaffung-von-redispatch.pdf?_blob=publicationFile&v=6.

[31] Steinke F, Wolfrum P, Hoffmann C. Grid vs. storage in a 100% renewable Europe. Renew Energy 2013;50:826–32. http://dx.doi.org/10.1016/j.renene.2012.07.044, URL: https://linkinghub.elsevier.com/retrieve/pii/S0960148112004818.

[32] Kamlage J-H, Drewing E, Reinermann JL, de Vries N, Flores M. Fighting fruitfully? Participation and conflict in the context of electricity grid extension in Germany. Util Policy 2020;64:101022. http://dx.doi.org/10.1016/j.jup.2020.101022, URL: https://linkinghub.elsevier.com/retrieve/pii/S0957178720300175.

[33] Pilpola S, Lund PD. Different flexibility options for better system integration of wind power. Energy Strategy Rev 2019;26:100368. http://dx.doi.org/10.1016/j.esr.2019.100368, URL: https://linkinghub.elsevier.com/retrieve/pii/S2211467X19300550.

[34] Brown T, Schlachtberger D, Kies A, Schramm S, Greiner M. Synergies of sector coupling and transmission reinforcement in a cost-optimised, highly renewable European energy system. Energy 2018;160:720–39. http://dx.doi.org/10.1016/j.energy.2018.06.222, URL: https://linkinghub.elsevier.com/retrieve/pii/S036054421831288X.

[35] Maruf MNI. Sector coupling in the north sea region—A review on the energy system modelling perspective. Energies 2019;12(22):4298. http://dx.doi.org/10.3390/en12224298, URL: https://www.mdpi.com/1996-1073/12/22/4298.

[36] Haumaier J, Hauser P, Hobbie H, Möst D. Grünes gas für die gaswirtschaft – Regionale power-to-gas-potentiale aus onshore-windenergie in deutschland. Z Energwirtsch 2020. http://dx.doi.org/10.1007/s12398-020-00274-w, URL: http://link.springer.com/10.1007/s12398-020-00274-w.

[37] Boudellal M. Power-to-gas: Renewable hydrogen economy for the energy transition. Berlin, Boston: De Gruyter; 2018, http://dx.doi.org/10.1515/9783110559811, URL: http://www.degruyter.com/view/books/9783110559811/9783110559811/9783110559811.xml.

[38] Thema M, Bauer F, Sterner M. Power-to-Gas: Electrolysis and methanation status review. Renew Sustain Energy Rev 2019;112:775–87. http://dx.doi.org/10.1016/j.rser.2019.06.030, URL: https://linkinghub.elsevier.com/retrieve/pii/S136403211930423X.

[39] Quarton CJ, Samsatli S. Power-to-gas for injection into the gas grid: What can we learn from real-life projects, economic assessments and systems modelling? Renew Sustain Energy Rev 2018;98:302–16. http://dx.doi.org/10.1016/j.rser.2018.09.007, URL: https://linkinghub.elsevier.com/retrieve/pii/S1364032118306531.

[41] Kopp M, Coleman D, Stiller C, Scheffer K, Aichinger J, Scheppat B. Energiepark mainz: Technical and economic analysis of the worldwide largest power-to-gas plant with PEM electrolysis. Int J Hydrogen Energy 2017;42(19):13311–20. http://dx.doi.org/10.1016/j.ijhydene.2016.12.145, URL: https://linkinghub.elsevier.com/retrieve/pii/S0360319917300083.

[42] Kuprat M, Bendig M, Pfeiffer K. Possible role of power-to-heat and power-to-gas as flexible loads in German medium voltage networks. Front Energy 2017;11(2):135–45. http://dx.doi.org/10.1007/s11708-017-0472-8, URL: http://link.springer.com/10.1007/s11708-017-0472-8.

[43] Schiebahn S, Grube T, Robinius M, Tietze V, Kumar B, Stolten D. Power to gas: Technological overview, systems analysis and economic assessment for a case study in Germany. Int J Hydrogen Energy 2015;40(12):4285–94. http://dx.doi.org/10.1016/j.ijhydene.2015.01.123, URL: https://linkinghub.elsevier.com/retrieve/pii/S0360319915001913.

[44] Milanzi S, Spiller C, Grosse B, Hermann L, Müller-Kirchenbauer J. Technischer stand und flexibilität des power-to-gas-verfahrens. Publisher: Zenodo; 2018, http://dx.doi.org/10.5281/ZENODO.2620254, URL: https://zenodo.org/record/2620254.

[45] Götz M, Lefebvre J, Mörs F, McDaniel Koch A, Graf F, Bajohr S, Reimert R, Kolb T. Renewable power-to-gas: A technological and economic review. Renew Energy 2016;85:1371–90. http://dx.doi.org/10.1016/j.renene.2015.07.066, URL: https://linkinghub.elsevier.com/retrieve/pii/S0960148115301610.

[46] Sterner M, Jentsch M, Holzhammer U. Energiewirtschaftliche und ökologische bewertung eines windgas-angebotes. 2011, URL: https://www.greenpeace-energy.de/fileadmin/docs/sonstiges/Greenpeace_Energy_Gutachten_Windgas_Fraunhofer_Sterner.pdf.

[47] Lehner M, Tichler R, Steinmüller H, Koppe M. Power-to-gas: Technology and business models. SpringerBriefs in Energy, Cham: Springer International Publishing; 2014, http://dx.doi.org/10.1007/978-3-319-03995-4, URL: http://link.springer.com/10.1007/978-3-319-03995-4.

[48] Salomone F, Giglio E, Ferrero D, Santarelli M, Pirone R, Bensaid S. Techno-economic modelling of a Power-to-Gas system based on SOEC electrolysis and CO2 methanation in a RES-based electric grid. Chem Eng J 2019;377:120233. http://dx.doi.org/10.1016/j.cej.2018.10.170, URL: https://linkinghub.elsevier.com/retrieve/pii/S1385894718321314.

[49] Schmidt M, Schwarz S, Stürmer B, Wagener L, Zuberbühler U. Technologiebericht 4.2a power-to-gas (methanisierung chemisch-katalytisch) innerhalb des forschungsprojekts tf_energiewende. 2018, URL: https://epub.wupperinst.org/frontdoor/deliver/index/docId/7059/file/7059_Power-to-gas.pdf.

[50] Zapf M. Power-to-gas – stand der technik und einsatzmöglichkeiten. In: Stromspeicher und power-to-gas im deutschen energiesystem. Wiesbaden: Springer Fachmedien Wiesbaden; 2017, p. 165–265. http://dx.doi.org/10.1007/978-3-658-15073-0_3, URL: http://link.springer.com/10.1007/978-3-658-15073-0_3.

[51] Gorre J, Ruoss F, Karjunen H, Schaffert J, Tynjälä T. Cost benefits of optimizing hydrogen storage and methanation capacities for Power-to-Gas plants in dynamic operation. Appl Energy 2020;257:113967. http://dx.doi.org/10.1016/j.apenergy.2019.113967, URL: https://linkinghub.elsevier.com/retrieve/pii/S030626191931654X.

[52] Gonzalez-Salazar MA, Kirsten T, Prchlik L. Review of the operational flexibility and emissions of gas- and coal-fired power plants in a future with growing renewables. Renew Sustain Energy Rev 2018;82:1497–513. http://dx.doi.org/10.1016/j.rser.2017.05.278, URL: https://linkinghub.elsevier.com/retrieve/pii/S1364032117309206.

[53] Kunz F, Zerrahn A. Coordinating cross-country congestion management. DIW Discussion Papers 1551, Berlin: Deutsches Institut für Wirtschaftsforschung (DIW); 2016, URL: http://hdl.handle.net/10419/129208.

[54] Kunz F. Improving congestion management: How to facilitate the integration of renewable generation in Germany. Energy J 2011;34(4). http://dx.doi.org/10.5547/01956574.34.4.4, URL: http://www.iaee.org/en/publications/ejarticle.aspx?id=2525.

[55] bdew. Branchenleitfaden: Vergütung von redispatch maßnahmen. 2018, URL: https://www.bdew.de/media/documents/Branchenleitfaden_Verguetung-von-Redispatch-Massnahmen.pdf.

[56] Kunz F, Weibezahn J, Hauser P, Heidari S, Schill W-P, Felten B, Kendziorski M, Zech M, Zepter J, von Hirschhausen C, Möst D, Weber C. Reference data set: Electricity, heat, and gas sector data for modeling the german system. Zenodo; 2017, http://dx.doi.org/10.5281/ZENODO.1044463, URL: https://zenodo.org/record/1044463. type: dataset.

[57] Weibezahn J, Kendziorski M. Illustrating the benefits of openness: A large-scale spatial economic dispatch model using the julia language. Energies 2019;12(6):1153. http://dx.doi.org/10.3390/en12061153, URL: https://www.mdpi.com/1996-1073/12/6/1153.

[58] Kunz F, Kendziorski M, Schill W-P, Weibezahn J, Zepter J, Hirschhausen CRv, Hauser P, Zech M, Möst D, Heidari S, Felten B, Weber C. Electricity, heat, and gas sector data for modeling the German system. DIW Data Documentation 92, Berlin: Deutsches Institut für Wirtschaftsforschung (DIW); 2017, URL: http://hdl.handle.net/10419/173388.

[59] Beran P, Pape C, Weber C. Modelling German electricity wholesale spot prices with a parsimonious fundamental model – Validation & application. Util Policy 2019;58:27–39. http://dx.doi.org/10.1016/j.jup.2019.01.008, URL: https://linkinghub.elsevier.com/retrieve/pii/S0957178719300359.

[60] BNetzA, BNetzA. Monitoringbericht 2016. Bericht, Bonn, Germany: Bundesnetzagentur; 2016, URL: https://www.bundesnetzagentur.de/SharedDocs/Mediathek/Monitoringberichte/Monitoringbericht2016.pdf.

[61] 50Hertz, Amprion, Tennet, Transnet BW. Netztransparenz redispatch. 2016, URL: https://www.netztransparenz.de/EnWG/Redispatch.

[62] 50Hertz, Amprion, TenneT, TransnetBW, 2020. Anhang zum Netzenwicklunsplan Strom 2030 Version 2019: Zweiter Entwurf. Technical Report. Germany. URL: https://www.netzentwicklungsplan.de/sites/default/files/paragraphs-files/NEP_Anhang_Aktualisierung_Januar_2020.pdf.

[63] Hirth L, Schlecht I, Maurer C, Tersteegen B. Kosten- oder marktbasiert? Zukünftige redispatch-beschaffung in deutschland. Technical Report, Germany: neue energieökonomik (neon), consentec, BMWi; 2019.

[64] Amprion, Europe, OG. hybdridge - Mit sektorenkopplung zur erfolgreichen energiewende. Technical Report, 2019, URL: https://www.hybridge.net/Dokumente/Downloads/Brosch%C3%BCren-und-Faltbl%C3%A4tter/DE/hybridge-Mit-Sektorenkopplung-zur-erfolgreichen-Energiewende.pdf.

[65] TenneT, Gasunie, Thyssengas. Gasunie, TenneT und Thyssengas steigen in konkrete planung für grüne sektorkopplung mit power-to-gas ein. 2018, URL: https://www.element-eins.eu/_Resources/Persistent/e7aa4af3a02e451eb43f6770275fd35211e62668/20181016_PM-Gasunie-TenneT-Thyssengas-Power-to-Gas-Pilot-Element1.pdf.